

A MODEL FOR THE TWO DIMENSIONAL INTERACTION
BETWEEN NON-LINEAR WAVES AND UNIFORM CURRENTS

CENTRE FOR NEWFOUNDLAND STUDIES

**TOTAL OF 10 PAGES ONLY
MAY BE XEROXED**

(Without Author's Permission)

SHAOWEN SONG



**A MODEL FOR THE TWO
DIMENSIONAL INTERACTION
BETWEEN NON-LINEAR WAVES AND
UNIFORM CURRENTS**

BY

©SHAOWEN SONG

A thesis submitted to the School of Graduate Studies in partial fulfillment of the requirements for the degree of Masters of Engineering

**FACULTY OF ENGINEERING AND APPLIED SCIENCE
MEMORIAL UNIVERSITY OF NEWFOUNDLAND**

October 1988

St. John's

Newfoundland

Canada

Permission has been granted to the National Library of Canada to microfilm this thesis and to lend or sell copies of the film.

The author (copyright owner) has reserved other publication rights, and neither the thesis nor extensive extracts from it may be printed or otherwise reproduced without his/her written permission.

L'autorisation a été accordée à la Bibliothèque nationale du Canada de microfilmer cette thèse et de prêter ou de vendre des exemplaires du film.

L'auteur (titulaire du droit d'auteur) se réserve les autres droits de publication; ni la thèse ni de longs extraits de celle-ci ne doivent être imprimés ou autrement reproduits sans son autorisation écrite.

ISBN 0-315-50469-2

Acknowledgements

The author wishes to extend his sincere appreciation for the help and guidance given by his supervisor, Dr. R. E. Baddour, during the work on this thesis.

The author would also like to thank the technical staff of Computer Services and the Faculty of Engineering Center for CAE at Memorial University for their help, consultation and the small turn-around time.

In closing, the author would like to express his gratitude to the School of Graduate Studies and the Faculty of Engineering and Applied Science for the financial assistance in the forms of fellowship and bursary.

Abstract

The interaction of water wave trains with a uniform current normal to the wave crests is considered. The combined wave-current motion resulting from the interaction is assumed stable and irrotational. The velocity potential, dispersion relation, the particle kinematics and pressure distribution upto the third order are developed. The conservation of mean mass, momentum and energy of the current-free wave, wave-free current and combined wave-current fields before and after the interaction are used, together with the dispersion relation on the free surface to derive a set of four nonlinear equations, through which the relationship between H, L, d, U and H_o, L_o, d_o, U_o is established, where H_o, L_o, d_o are respectively the current-free wave height, wave length, mean water depth, and U_o the wave-free current speed, H, L, d, U are respectively the wave height, wave length, water depth, current speed of the combined wave-current field after the interaction. This is a new approach to an old problem. A numerical method is used to solve the system of nonlinear equations to calculate H, L, d , and U when given the values of H_o, L_o, d_o and U_o . Numerical results for the changes of wave height, length, water depth, and current speed in the form of $H/H_o, L/L_o, \Delta d/d_o$, and $\Delta U/U_o$ are presented, where $\Delta d = d - d_o, \Delta U = U - U_o$. The prediction of the combined wave-current properties through H_o, L_o, d_o , and U_o is established by

using the velocity potential of the combined wave-current field and the numerical results of H , L , d , and U . A comparison between the experimental results of Thomas (1981) and the results of the present theory is presented, and surprising agreement is observed.

Discussions on the radiation stress and energy transfer in the combined wave-current field, and on the numerical method and precision control are given in the appendices.

Contents

1	Introduction	1
2	Literature Review	6
2.1	Two Dimensional Waves and Uniform Current Interaction	7
2.2	Interaction of Waves and Uniform Current at an Angle	10
2.3	Waves and Shear Current Interaction	12
3	Combined Wave-current Field	13
3.1	First order approximation	16
3.1.1	Potential function and dispersion relation	16
3.1.2	Properties of the first order wave-current field	19
3.2	Second order approximation	22
3.2.1	Potential function and dispersion relation	22
3.2.2	Properties of the second order wave-current field	28
3.3	Third order approximation	32
3.3.1	Potential function and dispersion relation	32
3.3.2	Properties of the third order wave-current field	36
4	Changes in Wave and Current	40
4.1	Conservation equations	41
4.2	Mean mass, momentum, energy fluxes	43
4.2.1	Fluxes in a current-free wave field	43

4.2.2	Fluxes in a wave-free current field	46
4.2.3	Fluxes in a wave-current field	47
4.3	Relationships between L , H , d , U and L_0 , H_0 , d_0 , U_0	51
4.4	Computational considerations and results	57
5	Prediction of the Combined Wave-Current Field Properties	63
6	Comparison Between Present Theory and Experiment	71
7	Conclusions and Recommendations for Further Research	80
	References	81
	Further Readings	87
	Appendices	93
A	A Discussion on the Radiation Stress and Energy Transfer in a wave-current Field	94
B	Numerical Considerations and Precision Control	100
C	Computer Program	103
D	Some Numerical Results	116

Notations

The following notations are used in this thesis:

- a — wave amplitude;
- a_x — horizontal particle acceleration;
- a_z — vertical particle acceleration;
- C — wave velocity;
- C_r — relative wave velocity;
- d — water depth;
- E_c — wave-free current energy flux;
- E_w — current-free wave energy flux;
- E_{wc} — combined wave-current field energy flux;
- g — acceleration due to gravity;
- H — wave height;
- K — wave number;
- L — wave length;

M_c	—	wave-free current momentum flux;
M_w	—	current-free wave momentum flux;
M_{wc}	—	combined wave current field momentum flux;
P	—	pressure;
Q_c	—	wave-free current mass flux;
Q_w	—	current-free wave mass flux;
Q_{wc}	—	combined wave current field mass flux;
T	—	wave period;
t	—	time;
U	—	current speed;
u	—	horizontal wave particle velocity;
w	—	vertical wave particle velocity;
x	—	horizontal axis;
z	—	vertical axis;
σ	—	wave frequency;
σ_r	—	relative wave frequency;
η	—	wave profile;

- ϕ_c — wave-free current field potential;
 ϕ_w — current-free wave field potential;
 Φ — combined wave-current field potential.

Parameters with (without) subscript "o" denote the value before (after) the interaction between the waves and the current.

List of Figures

- Fig. 4.1 Wave length ratio L/L_o vs current speed ratio U_o/C_o for plane wave parameters $a_o=0.75$ m, $L_o=100.0$ m, $d_o=25.0$ m.
- Fig. 4.2 Wave height ratio H/H_o vs current speed ratio U_o/C_o for plane wave parameters $a_o=0.75$ m, $L_o=100.0$ m, $d_o=25.0$ m.
- Fig. 4.3 Current change ratio $(U - U_o)/C_o$ vs current speed ratio U_o/C_o for plane wave parameters $a_o=0.75$ m, $L_o=100.0$ m, $d_o=25.0$ m.
- Fig. 4.4 Depth change ratio $(d - d_o)/d_o$ vs current speed ratio U_o/C_o for plane wave parameters $a_o=0.75$ m, $L_o=100.0$ m, $d_o=25.0$ m.
- Fig. 5.1 Maximum particle velocity distribution along water depth, for $U_o/C_o = -0.15$.
- Fig. 5.2 Maximum particle velocity distribution along water depth, for $U_o/C_o = -0.10$.
- Fig. 5.3 Maximum particle velocity distribution along water depth, for $U_o/C_o = -0.05$.
- Fig. 5.4 Maximum particle velocity distribution along water depth, for $U_o/C_o = 0.00$.
- Fig. 5.5 Maximum particle velocity distribution along water depth, for $U_o/C_o = 0.05$.

- Fig. 5.6 Maximum particle velocity distribution along water depth, for $U_o/C_o = 0.10$.
- Fig. 5.7 Maximum particle velocity distribution along water depth, for $U_o/C_o = 0.15$.
- Fig. 5.8 Maximum particle acceleration distribution along water depth, for $U_o/C_o = -0.15$.
- Fig. 5.9 Maximum particle acceleration distribution along water depth, for $U_o/C_o = -0.10$.
- Fig. 5.10 Maximum particle acceleration distribution along water depth, for $U_o/C_o = -0.05$.
- Fig. 5.11 Maximum particle acceleration distribution along water depth, for $U_o/C_o = 0.00$.
- Fig. 5.12 Maximum particle acceleration distribution along water depth, for $U_o/C_o = 0.05$.
- Fig. 5.13 Maximum particle acceleration distribution along water depth, for $U_o/C_o = 0.10$.
- Fig. 5.14 Maximum particle acceleration distribution along water depth, for $U_o/C_o = 0.15$.
- Fig. 5.15 Trajectories of particle at $z/d = -0.2$ in the wave-current field, for $U_o/C_o = -0.02$.
- Fig. 5.16 Trajectories of particle at $z/d = -0.2$ in the wave-current field, for $U_o/C_o = -0.01$.

- Fig. 5.17 Trajectories of particle at $z/d = -0.2$ in the wave-current field, for $\bar{U}_o/C_o = 0.01$.
- Fig. 5.18 Trajectories of particle at $z/d = -0.2$ in the wave-current field, for $\bar{U}_o/C_o = 0.02$.
- Fig. 6.1 Schematic section of the wind-wave-current flume in Hydraulics Laboratory used in Thomas experiments.
- Fig. 6.1 Comparison between the present theoretical predictions and Thomas(1981) experimental results for wave length changes.
- Fig. 6.2 Comparison between the present theoretical predictions and Thomas(1981) experimental results for wave height changes.
- Fig. 6.3 Comparison between the present theoretical predictions and Thomas(1981) experimental results for the wavelike horizontal particle velocity distribution along water depth, for $U_o = -59.7$ mm/s.
- Fig. 6.4 Comparison between the present theoretical predictions and Thomas(1981) experimental results for the wavelike horizontal particle velocity distribution along water depth, for $U_o = -116.2$ mm/s.
- Fig. 6.5 Comparison between the present theoretical predictions and Thomas(1981) experimental results for the wavelike horizontal particle velocity distribution along water depth, for $U_o = -159.8$ mm/s.
- Fig. 6.6 Comparison between the present theoretical predictions and Thomas(1981) experimental results for the wavelike horizontal particle velocity distribution along water depth, for $U_o = -203.0$ mm/s.

List of Tables

- Tab. 6.1 Comparison between the measured (Thomas 1981) and the predicted (present theory) wave length changes.
- Tab. 6.2 Comparison between the measured (Thomas 1981) and the predicted (present theory) wave height changes.
- Tab. 6.3 Predicted changes in current speed and mean water depth.
- Tab. D.1 Numerical results of wave length ratio L/L_0 .
- Tab. D.2 Numerical results of wave height ratio H/H_0 .
- Tab. D.3 Numerical results of current velocity change ratio $(U - U_0) \times 10^{-4}$.
- Tab. D.4 Numerical results of water depth change ratio $(d - d_0) \times 10^{-4}$.

Chapter 1

Introduction

Accounting for the action of environmental loads on structures is a typical task for coastal and ocean engineers. The theories for evaluating the loads induced by waves, wind and current have relatively been well developed. However, for that of the combined effect of wave and current have not. At present, most offshore design of drilling platforms and oil storage tanks is done on the design wave concept, that is, the forces predicted on the structure are associated with the maximum wave to be experienced by the structure during its lifetime. Quite often, the presence of oceanic or wind-driven currents is neglected in the design, or considered separately from the waves, while rarely would this quiescent condition exist. In fact, the presence of a current will significantly influence the wave action on structures. Two examples are mentioned here, showing the significant magnitude changes of the wave and wave force by the presence of a current. Schumann(1974, 1975) reports that in the Agulhas current near South Africa when the fully

developed sea waves with height of 6 m meet with this current the result may be giant waves with wave height of 18 m or even more. R.A. Dalrymple (1973) reports that if the maximum horizontal velocity due to the design wave is 16 fps, then the presence of a 2 fps current would increase the drag force on the structure by over 25%, even when the current velocity is small relative to the particle velocity induced by the wave motion. It is obvious, then, that rational offshore design must include the effect of currents.

Evaluating the combined wave-current forces depends on the well understanding of the wave-current interaction, namely the understanding of the changes of the wave and the current after the interaction and the modeling of the combined wave-current field formed by the wave and the current interaction. Theories for small amplitude waves interacting with a current have been developed, see, for example, Longuet-Higgins and Stewart (1960,1961), Dalrymple (1973). In these theories the changes in the current and the mean water depth induced by the interaction are neglected. It is the objective of this thesis to investigate higher order waves interaction with a current, to model the higher order wave-current field and to find the changes both in the wave and in the current, as well as in the mean water depth after the interaction.

In this thesis the interaction of two dimensional finite amplitude waves and a uniform current is studied; i.e. finite amplitude periodical waves on still water propagating into a wave-free, irrotational current in the same or

opposite direction of wave propagation, is considered. The process of the interaction between the wave and the current in this situation is assumed to be divided into three stages. In stage (1) the wave and the current field are assumed to exist separately. In stage (2) wave and current encounter each other and the interaction between the wave and the current takes place. This stage is an unstable one, since the wave and current characteristics change with time. After the interaction, in stage (3) a stable, uniform, irrotational wave-current field is assumed to be formed. It is for this combined wave-current field that the potential function, dispersion relation, particle kinematics, and pressure distribution up to the third order are developed. The corresponding physical situation and possible experimental set up is well described in Thomas (1981) and cited in Chapter 6 of this thesis. The results of the first order (see 3.1 of this thesis) developed by the approach of this thesis qualitatively compare well with that of previous studies, such as Longuet-Higgins and Stewart (1961). Furthermore, this approach could also be used to find the stream function solution of a wave and shear current field (S. Song and R.E. Baddour 1987, R.E. Baddour and S. Song 1988).

The relationship between the current-free wave length L_0 , wave height H_0 , wave-free current speed U_0 , mean water depth d , before the interaction and their counterparts, denoted without subscript "0", of the combined wave-current field is established by using the fundamental conservation relations for the mean rate of mass, momentum and energy transfer for the

considered fluid flows. Conservation of wave crests is also assumed, which implies that the wave period T remains constant. The energy exchange between the wave and the current is taken into account. Numerical results for the variation in L/L_0 , H/H_0 , $\Delta U/U_0$, and $\Delta d/d_0$ are presented. This is a new method for solving a well documented problem. Using this method not only the changes in the current and in the water depth could be calculated, but more importantly, the calculation of the changes in wave height and wave length is done by considering the changes in the current and in the depth, which should be considered when considering finite amplitude waves interaction with a current.

Comparison between the experimental results of Thomas (1981) and the results of the present theory for the wave length and height ratios, L/L_0 and H/H_0 respectively, and the wave particle velocity distribution are also presented, good agreement is generally observed.

The thesis is organized into seven chapters, four appendices, a list of references and a list of further readings. Following this introduction, Chapter 2 is a literature review on the wave-current interaction problem. Chapter 3 presents the velocity potential function, dispersion relation and other properties of the combined wave-current field upto the third order in wave amplitude. These properties are written in terms of the wave height H , wave length L , water depth d , and current speed U of the combined wave-current field. In chapter 4, the relationships between H , L , d , U , and

H_0 , L_0 , d_0 , U_0 are established by using the mean mass, momentum, energy conservation relations, as well as the dispersion relation. A numerical method is used to calculate H , L , d , U when given the values of H_0 , L_0 , d_0 , and U_0 . Chapter 5 contains the prediction of the combined wave-current field properties and the results of their computation for a range of values of the current ratio U_0/C_0 . A negative value for U_0/C_0 indicates a current opposing the current-free wave propagation. In chapter 6, a comparison between the experimental results of Thomas (1981) and the results of the present theory is presented. Chapter 7 contains conclusions and suggestions for future work. Appendix A contains a discussion on the radiation stress and the energy transfer in the combined wave-current field. Numerical considerations are discussed in Appendix B. The computer programs developed for the numerical solution of the nonlinear system of equations, and wave-current field properties calculation are listed in Appendix C. Appendix D gives some of the numerical results on the changes of wave length, wave height, current speed and the water depth.

Chapter 2

Literature Review

The effects of a following or opposing uniform current on the propagation of surface gravity waves were first discussed by Unna (1942) and Sverdrup (1944) and their investigations were basically on finding the changes in wave length and wave height kinematically. Johnson (1947) found the effects on waves which enter a uniform current at an angle and he suggested that "major ocean current, such as the Gulf Stream, may have an appreciable effect on the height, length, and direction of waves approaching the shore and under some circumstances may cause almost complete reflection." Arthur (1950) investigated the combined effect of nonuniform current and bottom topography of shallow water waves and made an application to waves entering an intense rip current. Sarpkaya (1957) investigated experimentally the height and length changes when oscillatory gravity waves propagated into flowing water. Tsao (1959) studied the wave interaction with a shear current.

Since 1960, the aspects of the interaction between gravity waves and a current motion have received increasing attention, covering a wide spectrum of problems ranging from studies on the combined wave-current field to changes in wave amplitude and wave length, etc. The works of Dalrymple (1973, 1975), Longuet-Higgins and Stewart (1960, 1961), Whitham (1962), Peregrine (1976), Jonsson and Skovgaard (1978), Brevik and Aas (1980), Thomas (1981) to name but a few, are already classics. The mechanism is intimately connected with the so-called radiation stress (Longuet-Higgins and Stewart 1960, 1964), wave action (Bretherton and Garret 1960, Jonsson 1978, Crapper 1984) as well as mean energy level (Jonsson 1978, and Jonsson, Brink-Kjaer and Thomas 1978).

In this chapter the existing theories are reviewed by classifying them under the following three topics:

1. Two dimensional waves and uniform current interaction;
2. Interaction of waves and uniform current at an angle;
3. Two dimensional waves and shear current interaction.

2.1 Two Dimensional Waves and Uniform Current Interaction

Wave interaction with a uniform current in the same or opposite direction, i.e. two dimensional-interaction, is a typical problem in the area of wave and current interaction. The purpose of the existing theories is mainly

to develop methods for determining the changes in wave length and wave height after the wave is affected by the current. Unna (1942) established a method to determine the changes in wave length and wave height by using the dispersion relation and the energy conservation equation given by the following two equations

$$C = C_r + U_o \quad (2.1)$$

and

$$E_o C_{g_o} = E(C_{g_r} + U_o) \quad (2.2)$$

where C , C_g , E and U are respectively the wave celerity, group velocity, wave energy density, and mean current speed; with the subscript "o" indicating the parameter before the wave train and current meet and subscript "r" indicating the relative value of the parameter.

By further assuming that $C_r = (\frac{gL}{2\pi} \tanh \frac{2\pi}{L} d)^{1/2}$ and $E = \frac{1}{8} \rho g H^2$, with d denoting the depth and H the wave height. The changes in wave-length and wave height were given as

$$\frac{L}{L_o} = (\sqrt{\frac{gL}{2\pi} \tanh \frac{2\pi}{L} d} + U_o) / (\sqrt{\frac{gL_o}{2\pi} \tanh \frac{2\pi}{L_o} d}) \quad (2.3)$$

and

$$\frac{H}{H_o} = 1 - \frac{U_o}{2C_o} \quad (2.4)$$

Longuet-Higgins and Stewart (1960, 1961, 1964) showed that there was no coupling between the waves and the current considered in Unna's

method. They found the change in wave height dynamically by considering this coupling. For small amplitude wave and current interaction, the change in wave height was given as

$$\frac{H}{H_0} = \left[\frac{C_0(C_0 + 2U_0)}{C(C + 2U)} \right]^{1/2} \quad (2.5)$$

Some special situations have also been studied such as the interaction of small amplitude waves with surface currents (Thomson and West 1975), wave and current interactions in shallow water (Yoon and Philip 1980) etc. Brevik and Aas (1980) review and study experimentally the amplitude variation when periodic waves, initially on still water, propagate into a known current fed from below. They identify a set down of the mean water surface because of the current, but the additional contribution to the set down because of the waves is, as they put it, completely negligible. The problem of waves propagating through a known slowly-varying, depth independent horizontal current is also reviewed by Craik (1985). Baddour and Song (1988) investigated the problem by considering the changes in the current as well as in the water depth.

Some experiments for special situations have also been reported by Sarpkaya (1957), Hughes and Stewart (1961), Huang, Chen and Tung (1972), Brevik and Aas (1980a, 1980b), Kemp and Simons (1982). G. P. Thomas (1981) studied the problem numerically and experimentally, and presented results on wave height and wave length, and the wave particle velocity

distribution in the wave-current field.

The objective of the present study is to investigate the interaction between steeper wave and a uniform current and to develop a method of calculating the changes both in the wave and current as well as in the mean water depth.

2.2 Interaction of Waves and Uniform Current at an Angle

When waves moving through still water encounter a current at an angle with the wave direction, the waves are refracted, undergoing changes in length, steepness and direction. Johnson (1947) discussed this problem by using ray theory. The dispersion relation was assumed to be

$$\frac{C_o}{\sin \alpha} = U_o + \frac{C_r}{\sin \beta} \quad (2.6)$$

where α is the initial angle between the incoming wave and current directions; β is the angle between the wave and current directions after the interaction.

From the ray theory it is known that

$$\frac{L}{\sin \beta} = \frac{L_o}{\sin \alpha} \quad (2.7)$$

Thus the changes in wave length, wave height, and in the angle could be found. They are given by the following equations

$$\frac{L}{L_0} = \frac{1}{(1 - M \sin \alpha)^2} \quad (2.8)$$

$$\frac{H}{H_0} = \frac{\cos \alpha (1 - M \sin \alpha)^3}{\cos \beta (1 + M \sin \alpha)} \left(\frac{\sin \beta}{\sin \alpha} \right)^2 \quad (2.9)$$

$$\sin \beta = \frac{\sin \alpha}{(1 - M \sin \alpha)^2} \quad (2.10)$$

where $M = U_0/C_0$.

Similarly, Jonsson and Skovgaard (1978) using the same theory studied the problem of waves propagating from current U_1 to current U_2 with an angle. The results were given as

$$L_2 = \frac{\sin \alpha_2}{\sin \alpha_1} L_1 \quad (2.11)$$

and

$$\frac{H_2}{H_1} = \sqrt{\frac{1 + G_1}{1 + G_2}} \sqrt{\frac{\sin 2\alpha_1}{\sin 2\alpha_2}} \quad (2.12)$$

where

$$G_2 = \frac{2K_1 d}{\sinh 2K_1 d} \quad (2.13)$$

$$G_2 = \frac{2K_2 d}{\sinh 2K_2 d} \quad (2.14)$$

with subscripts 1 and 2 denote the parameters related to U_1 and U_2 respectively.

Longuet-Higgins and Stewart (1960) also discussed this problem as an extension of their theory.

2.3 Waves and Shear Current Interaction

Wave interaction with a shear current is a more complicated problem, because of the nonpotential properties of the shear current. Therefore, investigation of this problem involves consideration of the stream function instead of the potential function, and only two dimensional situation has been studied. The existing theories on this topic mainly concentrated on finding the solution of the combined wave-shear current field instead of finding the changes in the wave length and wave height. The behavior of surface waves on a linearly varying current was first worked out by Tsao (1959). He gave the stream function and the dispersion relation of the wave-linear current field. Dalrymple (1973) studied the interaction of waves with a bilinear current, and made an attempt to analyse numerically waves and nonlinear current interactions. Song and Baddour(1987), Baddour and Song (1988b) investigated the problem of waves interaction with a linear current to the second order. Some work has also been done on treating special situations. Longuet-Higgins (1961) studied the problem of waves and current which varies gradually in the direction of wave propagation. Freeman and Johnson (1970) investigated the situation of shallow water waves on shear flows. Dennis (1973) analysed the problem of non-linear gravity-capillary surface waves in a slowly varying current.

Chapter 3

Combined Wave-current Field

As discussed in the introduction, the process of the interaction between a wave train and a current in the same or opposite direction of wave propagation is assumed to follow three stages. In stage one or the stage before the interaction the current-free waves and wave-free current are assumed to exist. In stage two, waves propagate into the current, and hence the interaction takes place. The waves and the current properties, as well as the water depth keep changing until finally a stable, combined wave-current field is assumed to be formed, which is here called the third stage or the stage after the interaction. It is for this combined wave-current field that the potential function, dispersion relation and other properties to the third order in wave amplitude are developed in this chapter.

The following assumptions are made:

1. The combined wave-current field is a two dimensional, irrotational and a stable one.

2. The fluid is assumed to be inviscid, incompressible and homogeneous.
3. The sea bottom is assumed to be horizontal and impermeable.

Since the combined wave-current field is assumed to be irrotational, a potential function exists and satisfies Laplace's equation, that is

$$\nabla^2 \Phi(x, z, t) = 0 \quad (3.1)$$

everywhere in the fluid domain where Φ denotes the potential function of the combined wave-current field.

Adopting a system of coordinates, with z vertically upwards, x horizontal, and the origin on the undisturbed free surface, the bottom boundary condition can be expressed as

$$\Phi_z = 0 \quad \text{on} \quad z = -d \quad (3.2)$$

where d is the mean constant water depth of the wave-current field and subscripts denote partial differentiation.

The kinematic free surface boundary condition is

$$\Phi_t = \eta_t + \Phi_z \eta_x \quad \text{on} \quad z = \eta(x, t) \quad (3.3)$$

where η is the profile of the surface elevation of the combined wave-current field.

The dynamic free surface boundary condition can be expressed as

$$g\eta + \Phi_t + \frac{1}{2}[(\Phi_x)^2 + (\Phi_z)^2] = F(t) \quad \text{on } z = \eta(x, t) \quad (3.4)$$

for some function $F(t)$ to be determined.

It is reasonable to assume that the function $\eta(x, t)$ describing the free surface elevation of the combined wave-current field is periodic and expressed in the form

$$\eta(x, t) = \sum_{m=0}^{\infty} a_m \cos m(Kx - \sigma t) \quad (3.5)$$

for some constants a_m to be evaluated, and where $K = 2\pi/L$ is the wave number, and σ is the frequency of the periodical motion. T is the period hence fixing σ as $2\pi/T$.

From the periodicity of η , it follows that $\Phi(x, z, t)$ could be assumed of the form

$$\Phi = A_0(z)x + \sum_{n=1}^{\infty} A_n(z) \sin n(Kx - \sigma t) \quad (3.6)$$

for the horizontal bottom case, where A_n , $n=0,1,2,\dots$, are functions of z only. Keeping one, two, three terms of the series in the expansions (3.5) and (3.6) are here called first, second or third order approximations, respectively.

3.1 First order approximation

3.1.1 Potential function and dispersion relation

Following a classical approach (see, for example, Lamb 1975) equations (3.3) and (3.4) are expanded in a Taylor series about $z = 0$. Keeping only the first order terms, yields the kinematic and the dynamic surface conditions

$$\Phi_z - \eta_t - \Phi_z \eta_z = 0 \quad (3.7)$$

and

$$g\eta + \Phi_t + \frac{1}{2}[(\Phi_x)^2 + (\Phi_z)^2] - F(t) = 0 \quad (3.8)$$

to be satisfied on $z = 0$

To the first order of approximation, the free surface elevation (3.5) and the potential function (3.6) are written as

$$\eta = a \cos(Kx - \sigma t) \quad (3.9)$$

and

$$\Phi = A_0(z)x + A_1(z) \sin(Kx - \sigma t) \quad (3.10)$$

where $a = H/2$ is the amplitude of the wave on the surface of the combined field, $A_0(z)$ and $A_1(z)$ are functions of z only.

By substituting equation (3.10) in equation (3.1) and by satisfying the bottom boundary condition (3.2), $A_0(z)$ and $A_1(z)$ can be found in the form

$$A_0(z) = B_0 \quad (3.11)$$

$$A_1(z) = B_1 \cosh K(z+d) \quad (3.12)$$

where B_0 and B_1 are constants to be determined. Equation (3.10) hence becomes

$$\Phi = B_0 x + B_1 \cosh K(z+d) \sin(Kx - \sigma t) \quad (3.13)$$

To determine B_1 , equations (3.9) and (3.13) are substituted into the free surface condition (3.8) and keeping terms upto the first order in a yields

$$\begin{aligned} B_1 K \sinh Kd \sin(Kx - \sigma t) - \\ - a\sigma \sin(Kx - \sigma t) + \\ + B_0 a K \sin(Kx - \sigma t) = 0 \end{aligned} \quad (3.14)$$

From equation (3.14) B_1 is found to be

$$B_1 = \frac{a}{\sinh Kd} (C - B_0) \quad (3.15)$$

where $C = \sigma/K$ is the absolute velocity of the surface disturbance of the wave-current field. The potential function Φ is hence of the form

$$\Phi = Ux + a(C - U) \frac{\cosh K(z+d)}{\sinh Kd} \sin(Kx - \sigma t) \quad (3.16)$$

where $U = B_0$ is the aperiodical part of the combined wave-current motion.

The dispersion relation of the surface wave is found by assuming $\partial P / \partial x = 0$, on $z = \eta$. Differentiating partially with respect to x , equation (3.8) gives

$$g \frac{\partial \eta}{\partial x} + \frac{\partial^2 \Phi}{\partial x \partial t} + \frac{1}{2} \frac{\partial}{\partial x} \left[\left(\frac{\partial \Phi}{\partial x} \right)^2 + \left(\frac{\partial \Phi}{\partial z} \right)^2 \right] = 0 \quad (3.17)$$

Substituting equations (3.9) and (3.16) into (3.17) and keeping the first order terms yields

$$\begin{aligned} & -gaK \sin(Kx - \sigma t) + \\ & + a(C - U)K\sigma \coth Kd \sin(Kx - \sigma t) - \\ & - Ua(C - U)K^2 \coth Kd \sin(Kx - \sigma t) = 0 \end{aligned} \quad (3.18)$$

From equation (3.18) the following quadratic equation can be obtained

$$(C - U)^2 - \frac{g}{K} \tanh Kd = 0 \quad (3.19)$$

Solving equation (3.19) yields the dispersion relation of the combined wave-current field to be

$$C = U \pm C_r \quad (3.20)$$

where $C_r = [(g/K) \tanh Kd]^{1/2} = \sigma_r/K$ is the celerity relative to the current stream U and σ_r is the relative frequency. Equation (3.20) is known as the Doppler relation.

$F(t)$ in Bernoulli's equation (3.8) is found, by substituting for η and Φ in equation (3.8), as

$$F(t) = \frac{1}{2}U^2 \quad (3.21)$$

3.1.2 Properties of the first order wave-current field

The properties of the combined wave-current field to the first order of approximation can be derived from the first order potential function and the dispersion relation. They are listed below.

- 1). The velocity potential is given by (3.16)

$$\Phi = Ux + a(C_r - U) \frac{\cosh K(z+d)}{\sinh Kd} \sin(Kx - \sigma t) \quad (3.22)$$

- 2). The dispersion relation was found to be

$$C = U \pm C_r \quad (3.23)$$

where

$$C_r = \left(\frac{g}{K} \tanh Kd\right)^{1/2} = \sigma_r / K \quad (3.24)$$

and σ_r is the relative wave frequency.

3). Particle velocity

The x and z components of particle velocity $\vec{V} = \nabla\Phi$ in the combined field are respectively given by

$$u = U + \frac{gaK \cosh K(z+d)}{\sigma_r \cosh Kd} \cos(Kx - \sigma t) \quad (3.25)$$

$$w = \frac{gaK \sinh K(z+d)}{\sigma_r \cosh Kd} \sin(Kx - \sigma t) \quad (3.26)$$

4). Particle acceleration

The x and z components of particle acceleration

$$\vec{a} = \frac{D\vec{V}}{Dt} = \left(\frac{\partial}{\partial t} + \vec{V} \cdot \nabla\right)\vec{V} \quad (3.27)$$

in the combined field could be obtained in the form

$$a_x = gaK \frac{\cosh K(z+d)}{\cosh Kd} \sin(Kx - \sigma t) \quad (3.28)$$

$$a_z = -gaK \frac{\sinh K(z+d)}{\cosh Kd} \cos(Kx - \sigma t) \quad (3.29)$$

5). Particle path

To find the particle trajectory in the wave-current field, equations (3.25) and (3.26) at a certain point (x_i, z_i) are integrated with respect to time t to yield

$$x = x_i + Ut - a \frac{\cosh K(z_i + d)}{\sinh Kd} \sin(Kx_i - \sigma t) \quad (3.30)$$

$$z = z_i + a \frac{\sinh K(z_i + d)}{\sinh Kd} \cos(Kx_i - \sigma t) \quad (3.31)$$

Combining equations (3.30) and (3.31) the path of the particle can also be written as

$$\frac{(z - z_i)^2}{\alpha^2} + \frac{(x - x_i - Ut)^2}{\beta^2} = 1 \quad (3.32)$$

where

$$\alpha = \frac{a \sinh K(z_i + d)}{\sinh Kd} \quad (3.33)$$

$$\beta = \frac{a \cosh K(z_i + d)}{\sinh Kd} \quad (3.34)$$

6). Pressure distribution

The pressure distribution in a potential flow is given by Bernoulli's equation in the form

$$P = -\rho g z - \rho \frac{\partial \Phi}{\partial t} - \frac{\rho}{2} \left[\left(\frac{\partial \Phi}{\partial x} \right)^2 + \left(\frac{\partial \Phi}{\partial z} \right)^2 \right] + \rho F(t) \quad (3.35)$$

Substituting $F(t)$ and Φ from equations (3.21) and (3.22) in (3.35), the pressure distribution in a combined wave-current field to the first order of approximation could then be obtained in the form

$$P = -\rho g z + \rho \frac{K a}{\sinh K d} (C - U)^2 \cosh K(x + d) \cos(Kx - \sigma t) \quad (3.36)$$

3.2 Second order approximation

3.2.1 Potential function and dispersion relation

Keeping the second order terms in expressions (3.5) and (3.6) for the surface elevation and the potential function, gives the second approximation to the wave-current field as

$$\eta = a_1 \cos(Kx - \sigma t) + a_2 \cos 2(Kx - \sigma t) \quad (3.37)$$

and

$$\Phi = A_0(z)x + A_1(z) \sin(Kx - \sigma t) + A_2(z) \sin 2(Kx - \sigma t) \quad (3.38)$$

Substituting equation (3.38) into the governing equation (3.1) the following system of ordinary differential equations could be obtained

$$A_0''(z) = 0 \quad (3.39)$$

$$A_1''(z) - K^2 A_1(z) = 0 \quad (3.40)$$

$$A_2''(z) - 4K^2 A_2(z) = 0 \quad (3.41)$$

Equations (3.39), (3.40) and (3.41) describe a system of ordinary differential equations, to be solved for $A_0(z)$, $A_1(z)$ and $A_2(z)$. A prime denotes differentiation with respect to z .

The bottom boundary condition (3.2) implies that

$$A_0'(z) = 0 \quad \text{on} \quad z = -d \quad (3.42)$$

$$A_1'(z) = 0 \quad \text{on} \quad z = -d \quad (3.43)$$

and

$$A_2'(z) = 0 \quad \text{on} \quad z = -d \quad (3.44)$$

which on solving equations (3.39), (3.40) and (3.41), suggest the form of the functions $A_0(z)$, $A_1(z)$, $A_2(z)$ for any constant K , as

$$A_0(z) = B_0 \quad (3.45)$$

$$A_1(z) = B_1 \cosh K(z+d) \quad (3.46)$$

$$A_2(z) = B_2 \cosh 2K(z+d) \quad (3.47)$$

for some constants B_0, B_1, B_2 to be determined. Hence formally Φ is, to second order, written in the form

$$\Phi = B_0 x + B_1 \cosh K(z+d) \sin(Kx - \sigma t) + B_2 \cosh 2K(z+d) \sin 2(Kx - \sigma t) \quad (3.48)$$

Now expanding equation (3.3) in a Taylor's series about $z = 0$ and keeping terms up to the second order, yields the second order kinematic surface condition

$$\frac{\partial \Phi}{\partial x} - \frac{\partial \eta}{\partial t} - \frac{\partial \Phi}{\partial x} \frac{\partial \eta}{\partial x} + \frac{\partial^2 \Phi}{\partial z^2} \eta - \frac{\partial^2 \Phi}{\partial x \partial z} \frac{\partial \eta}{\partial x} = 0 \quad (3.49)$$

to be satisfied on $z = 0$.

Substituting equations (3.37) and (3.48) for η and Φ , in equation (3.49) yields

$$\begin{aligned}
 & B_1 K \sinh Kd - a_1 \sigma + a_1 K B_0 + \\
 & + a_2 B_1 K^2 \cosh Kd - a_1 B_2 K^2 \cosh 2Kd + \\
 & + 2a_1 B_2 K^2 \cosh 2Kd - \frac{1}{2} a_2 B_1 K^2 \cosh Kd - \\
 & - \frac{1}{2} a_1^2 B_1 K^3 \sinh Kd = 0 \quad (3.50)
 \end{aligned}$$

and

$$\begin{aligned}
 & 2B_2 K \sinh 2Kd - 2a_2 \sigma + 2a_2 K B_0 + \\
 & + \frac{1}{2} a_1 K^2 B_1 \cosh Kd + \frac{1}{2} a_1 B_1 K^2 \cosh Kd = 0 \quad (3.51)
 \end{aligned}$$

On solving equations (3.50) and (3.51) the coefficients B_1 and B_2 are determined to be

$$B_1 = \frac{a_1(C - B_0)}{\sinh Kd} \quad (3.52)$$

and

$$B_2 = \frac{(C - B_0)}{\sinh 2Kd} \left[a_2 - \frac{1}{2} a_1^2 K \coth Kd \right] \quad (3.53)$$

For the same reason as for the first order, setting $B_0 = U$ and substituting (3.52) and (3.53) back in equation (3.48) the potential function to the second order is expressed as

$$\begin{aligned}
\Phi = & Ux + \frac{a_1(C-U)}{\sinh Kd} \cosh K(z+d) \sin(Kx - \sigma t) + \\
& + \frac{(C-U)}{\sinh 2Kd} \left[a_2 - \frac{1}{2} a_1^2 K \coth Kd \right] \cdot \\
& \cdot \cosh 2K(z+d) \sin 2(Kx - \sigma t)
\end{aligned} \tag{3.54}$$

Also expanding equation (3.4) in a Taylor's series about $z = 0$ to the second order yields the dynamic free surface condition in the form

$$\begin{aligned}
g\eta + \frac{\partial \Phi}{\partial t} + \frac{1}{2} \left[\left(\frac{\partial \Phi}{\partial x} \right)^2 + \left(\frac{\partial \Phi}{\partial z} \right)^2 \right] - F(t) + \\
\frac{\partial^2 \Phi}{\partial t \partial z} \eta + \frac{\partial \Phi}{\partial x} \frac{\partial^2 \Phi}{\partial x \partial z} \eta + \frac{\partial \Phi}{\partial z} \frac{\partial^2 \Phi}{\partial z^2} \eta = 0
\end{aligned} \tag{3.55}$$

to be satisfied on $z = 0$.

Differentiating equation (3.55) partially with respect to x gives.

$$\begin{aligned}
& \frac{\partial \eta}{\partial x} + \frac{\partial^2 \Phi}{\partial t \partial x} + \frac{\partial \Phi}{\partial x} \frac{\partial^2 \Phi}{\partial x^2} + \frac{\partial \Phi}{\partial x} \frac{\partial^2 \Phi}{\partial x \partial z} + \\
& + \frac{\partial^3 \Phi}{\partial t \partial z \partial x} \eta + \frac{\partial \eta}{\partial x} \frac{\partial^2 \Phi}{\partial t \partial z} + \frac{\partial^2 \Phi}{\partial x^2} \frac{\partial^2 \Phi}{\partial x \partial z} \eta + \\
& + \frac{\partial \Phi}{\partial x} \frac{\partial^3}{\partial x^2 \partial z} \eta + \frac{\partial \Phi}{\partial x} \frac{\partial^2 \Phi}{\partial x \partial z} \frac{\partial \eta}{\partial x} + \\
& + \frac{\partial^2 \Phi}{\partial z \partial x} \frac{\partial^2 \Phi}{\partial x^2} \eta + \frac{\partial \Phi}{\partial z} \frac{\partial^3 \Phi}{\partial x^2 \partial x} \eta + \\
& + \frac{\partial \Phi}{\partial z} \frac{\partial^2 \Phi}{\partial x^2} \frac{\partial \eta}{\partial x} = 0 \quad (3.56)
\end{aligned}$$

On substituting equation (3.37) and (3.54) into equation (3.56) the dispersion relation and the second order term amplitude a_2 could be found to be

$$C = U \pm C_r \quad (3.57)$$

where

$$C_r = \left(\frac{g}{K} \tanh Kd \right)^{1/2} \quad (3.58)$$

and

$$a_2 = \frac{\pi H^2}{4L} \left(1 + \frac{3}{2 \sinh^2 Kd}\right) \coth Kd \quad (3.59)$$

where $H = 2a_1$ is the wave height for the first order wave amplitude a_1 .

It is worth noting that the dispersion relation of the second order approximation is the same as the first order one. This is in agreement with the Stokes's second order wave theory for the special case when the current speed U is zero.

Bernoulli's equation constant $F(t)$ is found to be

$$F(t) = \frac{1}{2}U^2 + \frac{1}{2}a^2Kg \frac{1}{\sinh 2Kd} \quad (3.60)$$

3.2.2 Properties of the second order wave-current field

For convenience the properties of the second order wave current field are listed below. In the following a , without a subscript 1, is used to denote the first order amplitude.

1). Potential function is

$$\begin{aligned} \Phi = & Ux + a(C - U) \frac{\cosh K(z+d)}{\sinh Kd} \sin(Kx - \sigma t) + \\ & + [a_2 - \frac{1}{2}a^2K \coth Kd](C - U) \cdot \\ & \frac{\cosh 2K(z+d)}{\sinh 2Kd} \sin 2(Kx - \sigma t) \end{aligned} \quad (3.61)$$

where



$$a_2 = \frac{\pi a^2}{L} \left(1 + \frac{3}{2 \sinh^2 Kd} \right) \coth Kd \quad (3.62)$$

and $a = H/2$, H is the wave height of the combined wave-current field.

2) Free surface profile is

$$\eta = a \cos(Kx - \sigma t) + a_2 \cos 2(Kx - \sigma t) \quad (3.63)$$

3). Dispersion relation is given by

$$C = U \pm C_r \quad (3.64)$$

and

$$C_r = \left(\frac{g}{K} \tanh Kd \right)^{1/2} \quad (3.65)$$

4). Particle velocity

The components of particle velocity are given by

$$u = U + \frac{gaK \cosh K(z+d)}{\sigma_r \cosh Kd} \cos(Kx - \sigma t) + \frac{3a^2 K \sigma_r}{4 \sinh^4 Kd} \cosh 2K(z+d) \cos 2(Kx - \sigma t) \quad (3.66)$$

$$w = \frac{gaK}{\sigma_r} \frac{\sinh K(z+d)}{\cosh Kd} \sin(Kx - \sigma t) + \frac{3}{4} \frac{a^2 K \sigma_r}{\sinh^4 Kd} \sinh 2K(z+d) \sin 2(Kx - \sigma t) \quad (3.67)$$

where the relative frequency is defined by

$$\sigma_r = (Kg \tanh Kd)^{1/2}. \quad (3.68)$$

5). Particle acceleration

The x and z components of particle acceleration are, to second order, given by

$$a_x = gaK \frac{\cosh K(z+d)}{\cosh Kd} \sin(Kx - \sigma t) + \left[\frac{3}{2} \frac{a^2 K \sigma_r^2}{\sinh^4 Kd} \cosh 2K(z+d) - \frac{ga^2 K^2}{\sinh 2Kd} \right] \sin 2(Kx - \sigma t) \quad (3.69)$$

$$a_z = ga^2 K^2 \frac{\sinh 2K(z+d)}{\sinh 2Kd} - gaK \frac{\sinh K(z+d)}{\cosh Kd} \cos(Kx - \sigma t) - \frac{3}{2} \frac{a^2 K \sigma_r^2}{\sinh^4 Kd} \sinh 2K(z+d) \cos 2(Kx - \sigma t) \quad (3.70)$$

6). Particle path

The trajectory of a particle, initially located at (x_i, z_i) in the combined wave-current field, is described, to second order by the parametric equations

$$x = x_i + Ut - a \frac{\cosh K(z_i + d)}{\sinh Kd} \sin(Kx_i - \sigma_r t) - \frac{3}{8} \frac{a^2 K}{\sinh^4 Kd} \cosh 2K(z_i + d) \sin 2(Kx_i - \sigma_r t) \quad (3.71)$$

$$z = z_i + a \frac{\sinh K(z_i + d)}{\sinh Kd} \cos(Kx_i - \sigma_r t) + \frac{3}{8} \frac{a^2 K}{\sinh^4 Kd} \sinh 2K(z_i + d) \cos 2(Kx_i - \sigma_r t) \quad (3.72)$$

7). Pressure distribution

The pressure distribution in the combined wave-current field is, to the second order, given by

$$P = -\rho g z - \frac{1}{2} \rho g K a^2 \frac{1}{\sinh 2Kd} [\cosh 2K(z+d) - 1] + \rho g a \frac{\cosh K(z+d)}{\cosh Kd} \cos(Kx - \sigma t) + \frac{3}{2} \rho g K a^2 \frac{1}{\sinh 2Kd} \left[\frac{\cosh 2K(z+d)}{\sinh^2 Kd} - \frac{1}{3} \right] \cos 2(Kx - \sigma t) \quad (3.73)$$

3.3 Third order approximation

3.3.1 Potential function and dispersion relation

In the same way as in sections (3.1) and (3.2), keeping third order terms in expressions (3.5) and (3.6), gives the third order approximation of the surface elevation and the potential function of the combined wave-current field in the form

$$\eta = a_1 \cos(Kx - \sigma t) + a_2 \cos 2(Kx - \sigma t) + a_3 \cos 3(Kx - \sigma t) \quad (3.74)$$

$$\Phi = A_0(z)x + A_1(z) \sin(Kx - \sigma t) + A_2(z) \sin 2(Kx - \sigma t) + A_3(z) \sin 3(Kx - \sigma t) \quad (3.75)$$

Through the same procedure as for the first and second order approximations, $A_0(z)$, $A_1(z)$, $A_2(z)$, $A_3(z)$ in (3.75) are found, on solving a corresponding system of ordinary differential equations, to be

$$A_0(z) = B_0 \quad (3.76)$$

$$A_1(z) = B_1 \cosh K(z + d) \quad (3.77)$$

$$A_2(z) = B_2 \cosh 2K(z+d) \quad (3.78)$$

$$A_3(z) = B_3 \cosh 3K(z+d) \quad (3.79)$$

for some constants B_0, B_1, B_2 and B_3 .

Thus Φ could be written in the form

$$\begin{aligned} \Phi = & B_0 x + B_1 \cosh K(z+d) \sin(Kx - \sigma t) + \\ & + B_2 \cosh 2K(z+d) \sin 2(Kx - \sigma t) + \\ & + B_3 \cosh 3K(z+d) \sin 3(Kx - \sigma t) \end{aligned} \quad (3.80)$$

Again, expanding the free surface kinematic and dynamic conditions in Taylor's expansion about $z = 0$ upto the third order terms gives respectively

$$\begin{aligned} \frac{\partial \Phi}{\partial z} - \frac{\partial \eta}{\partial t} + \frac{\partial \Phi}{\partial x} \frac{\partial \eta}{\partial x} + \frac{\partial^2 \Phi}{\partial z^2} \eta - \\ - \frac{\partial^2 \Phi}{\partial x \partial z} \frac{\partial \eta}{\partial x} + \frac{1}{2} \frac{\partial^3 \Phi}{\partial z^3} \eta^2 - \\ - \frac{1}{2} \frac{\partial^3 \Phi}{\partial x \partial z^2} \frac{\partial \eta}{\partial x} \eta^2 = 0 \end{aligned} \quad (3.81)$$

and

$$\begin{aligned}
& g\eta + \frac{\partial\Phi}{\partial t} + \frac{1}{2}\left[\left(\frac{\partial\Phi}{\partial x}\right)^2 + \left(\frac{\partial\Phi}{\partial z}\right)^2\right] - \\
& - F(t) + \frac{\partial^2\Phi}{\partial t\partial z}\eta + \frac{\partial\Phi}{\partial x}\frac{\partial^2\Phi}{\partial x\partial z} + \\
& + \frac{\partial\Phi}{\partial z}\frac{\partial^2\Phi}{\partial z^2}\eta + \frac{1}{2}\eta^2\left[\frac{\partial^3\Phi}{\partial t\partial z^2} + \left(\frac{\partial^2\Phi}{\partial x\partial z}\right)^2 + \right. \\
& \left. + \frac{\partial\Phi}{\partial x}\frac{\partial^3\Phi}{\partial x\partial z^2} + \left(\frac{\partial^2\Phi}{\partial z^2}\right)^2 + \frac{\partial\Phi}{\partial z}\frac{\partial^3\Phi}{\partial z^3}\right] = 0 \quad (3.82)
\end{aligned}$$

to be satisfied on $z = 0$.

By satisfying equations (3.81) and (3.82) to all considered orders the coefficients $a_m, m=1,2,3$; $B_n, n=1,2,3$; the dispersion relation, and function $F(t)$ could be found, in terms of the first order amplitude a_1 and uniform current-like speed U , to be

$$a_2 = \frac{1}{4}Ka^2 \frac{(2 + \cosh 2Kd)}{\sinh^3 Kd} \cosh Kd \quad (3.83)$$

$$a_3 = \frac{3}{64}K^2 a^3 \frac{1 + 8 \cosh^6 Kd}{\sinh^6 Kd} \quad (3.84)$$

$$B_0 = U \quad (3.85)$$

$$B_1 = \frac{a\sigma_r}{K \sinh Kd} \quad (3.86)$$

$$B_2 = \frac{3}{8} a^2 \sigma_r \frac{1}{\sinh^4 Kd} \quad (3.87)$$

$$B_3 = \frac{1}{64} \sigma_r K a^3 \left(\frac{11 - 2 \cosh 2Kd}{\sinh^7 Kd} \right) \quad (3.88)$$

$$C = U \pm \frac{\sigma_r}{K} \quad (3.89)$$

where

$$\sigma_r = \sqrt{Kg \tanh Kd [1 + (Ka)^2 \frac{8 + \cosh 4Kd}{8 \sinh^4 Kd}]^{1/2}}, \quad (3.90)$$

and

$$F(t) = \frac{1}{2} U^2 + \frac{1}{2} a^2 K g \frac{1}{\sinh 2Kd} \quad (3.91)$$

The surface wave height H in this case is given by

$$H = 2(a + a_3). \quad (3.92)$$

Note that a is used to denote the first order amplitude a_1 .

3.3.2 Properties of the third order wave-current field

As in sections (3.1.2) and (3.2.2) the properties of the third order wave-current field are listed below for completeness. The expressions are just more complicated.

1). Potential function

The potential is, to the third order, given by

$$\begin{aligned} \Phi = & Ux + \frac{a\sigma_r}{K \sinh Kd} \cosh K(z+d) \sin(Kx - \sigma t) + \\ & + \frac{3}{8} \frac{a^2 \sigma_r}{\sinh^4 Kd} \cosh 2K(z+d) \sin 2(Kx - \sigma t) + \\ & + \frac{1}{64} K \sigma_r a^3 \left(\frac{11 - 2 \cosh 2Kd}{\sinh^7 Kd} \right) \\ & \cosh 3K(z+d) \sin 3(Kx - \sigma t) \end{aligned} \quad (3.93)$$

where σ_r is given by equation (3.90).

2). Free surface profile

The free surface profile to third order is

$$\begin{aligned} \eta = & a \cos(Kx - \sigma t) + \\ & + \frac{a^2 K (2 + \cosh 2Kd) \cosh Kd}{4 \sinh^3 Kd} \cos 2(Kx - \sigma t) + \\ & + \frac{3}{64} K^2 a^3 \frac{(1 + 8 \cosh^6 Kd)}{\sinh^6 Kd} \cos 3(Kx - \sigma t) \end{aligned} \quad (3.94)$$

3). Dispersion relation

$$C = U \pm \sqrt{\frac{g}{K} \tanh Kd \left[1 + (Ka)^2 \frac{8 + \cosh 4Kd}{8 \sinh^4 Kd} \right]^{1/2}} \quad (3.95)$$

4). Particle velocity

To third order the velocity components of a particle are

$$\begin{aligned} u = & U + \frac{a\sigma_r}{\sinh Kd} \cosh K(z+d) \cos(Kx - \sigma t) + \\ & + \frac{3}{4} \frac{K\sigma_r a^2}{\sinh^4 Kd} \sinh 2K(z+d) \cos 2(Kx - \sigma t) + \\ & + \frac{3}{64} K^2 \sigma_r a^3 \frac{11 - 2 \cosh 2Kd}{\sinh^7 Kd} \\ & \cosh 3K(z+d) \cos 3(Kx - \sigma t) \end{aligned} \quad (3.96)$$

$$\begin{aligned} w = & \frac{a\sigma_r}{\sinh Kd} \sinh K(z+d) \sin(Kx - \sigma t) + \\ & + \frac{3}{4} \frac{K\sigma_r a^2}{\sinh^4 Kd} \sinh 2K(z+d) \sin 2(Kx - \sigma t) + \\ & + \frac{3}{64} K^2 \sigma_r a^3 \frac{11 - 2 \cosh 2Kd}{\sinh^7 Kd} \\ & \sinh 3K(z+d) \sin 3(Kx - \sigma t) \end{aligned} \quad (3.97)$$

5). Particle acceleration

Also the components of acceleration can be written as

$$\begin{aligned}
a_x = & \{f_1 \sigma_r \cosh K(z+d) - \\
& - \frac{1}{2} f_1 f_2 K [\sinh K(z+d) \sinh 2K(z+d) + \\
& + \cosh K(z+d) \cosh 2(z+d)] \sin(Kx - \sigma t) + \\
& + [2f_2 \sigma_r \cosh 2K(z+d) - \frac{1}{2} f_1^2 K] \sin 2(Kx - \sigma t) + \\
& + [3f_3 \sigma_r \cosh 3K(z+d) + \\
& + \frac{3}{2} f_1 f_2 K [\sinh K(z+d) \sinh 2K(z+d) - \\
& - \cosh K(z+d) \cosh 2K(z+d)] \sin 3(Kx - \sigma t) \} \quad (3.98)
\end{aligned}$$

$$\begin{aligned}
a_x = & f_1^2 K \sinh K(z+d) \cosh K(z+d) - \\
& - \{f_1 \sigma_r \sinh K(z+d) - \\
& - \frac{3}{2} f_1 f_2 K [\sinh K(z+d) \cosh 2K(z+d) + \\
& + \cosh K(z+d) \sinh 2K(z+d)] \cos(Kx - \sigma t) - \\
& - 2f_2 \sigma_r \sinh 2K(z+d) \cos 2(Kx - \sigma t) - \\
& - [3f_3 \sigma_r \sinh 3K(z+d) - \\
& - \frac{1}{2} f_1 f_2 K [\cosh K(z+d) \sinh 2K(z+d) - \\
& - \sinh K(z+d) \cosh 2K(z+d)] \cos 3(Kx - \sigma t) \} \quad (3.99)
\end{aligned}$$

where

$$f_1 = \frac{a\sigma_r}{\sinh Kd} \quad (3.100)$$

$$f_2 = \frac{3}{4} \frac{K\sigma_r a^2}{\sinh^4 Kd} \quad (3.101)$$

$$f_3 = \frac{3}{64} K^2 \sigma_r a^3 \frac{11 - 2 \cosh 2Kd}{\sinh^7 Kd} \quad (3.102)$$

6). Pressure distribution

The pressure is given to third order as

$$\begin{aligned} P = & -\rho g z - \frac{1}{4} \rho f_1^2 [\cosh 2K(z+d) - 1] + \\ & + \rho \left\{ f_1 \frac{\sigma_r}{K} \cosh K(z+d) + \right. \\ & + \frac{1}{2} f_1 f_2 [\sinh K(z+d) \sinh 2K(z+d) + \\ & + \cosh K(z+d) \cosh 2K(z+d)] \} \cos(Kx - \sigma t) + \\ & + \rho \left\{ f_2 \frac{\sigma_r}{K} \cosh 2K(z+d) - \frac{1}{4} f_1^2 \right\} \cos 2(Kx - \sigma t) + \\ & + \rho \left\{ f_3 \frac{\sigma_r}{K} \cosh 3K(z+d) + \right. \\ & + \frac{1}{2} f_1 f_2 [\sinh K(z+d) \sinh 2K(z+d) \\ & - \cosh K(z+d) \cosh 2K(z+d)] \} \cos 3(Kx - \sigma t) \quad (3.103) \end{aligned}$$

where f_1 , f_2 , f_3 are expressed above by (3.100), (3.101), (3.102) respectively.

Chapter 4

Changes in Wave and Current

In the previous chapter the solution and the properties of the combined wave-current field have been developed in terms of the surface disturbance wave length L , wave height H , water depth d , and uniform current speed U of the combined wave-current field. Since the current-free wave and wave-free current undergo changes after the interaction, L , H , d , U will be different from the length L_0 , height H_0 , water depth d_0 , and current speed U_0 of the current-free wave and wave-free current through which the combined wave-current field is formed (a subscript "0" is used in this thesis to denote the parameters before the wave-current interaction). It is the objective of the present section to find the relation between L, H, d, U and L_0, H_0, d_0, U_0 and to describe a method to calculate L, H, d, U knowing the values of L_0, H_0, d_0 , and U_0 .

4.1 Conservation equations

From a general point of view in a fluid, the mass, momentum and energy conservation relations are respectively given by

$$\int_s \rho(\vec{V} \cdot \vec{n}) ds + \frac{\partial}{\partial t} \int_r \rho d\tau = 0 \quad (4.1)$$

$$\int_r \rho \vec{F} d\tau + \int_s \vec{P}_s ds - \int_s \rho(\vec{V} \cdot \vec{n}) \vec{V} ds - \frac{\partial}{\partial t} \int_r \rho \vec{V} d\tau = 0 \quad (4.2)$$

$$\int_s (P + \frac{1}{2} \rho V^2 - \rho g z)(\vec{V} \cdot \vec{n}) ds = 0 \quad (4.3)$$

where \vec{n} denotes the unit vector normal to and directed from inside to outside of the fixed control surface s in the fluid domain enclosing a volume τ of fluid, with z axis vertically upwards.

\vec{V} , \vec{F} and \vec{P}_s denote respectively the velocity vector, the fluid body force per unit volume and surface force per unit area. For an incompressible, inviscid fluid steady flow under gravity, the above equations take the form

$$\int_s \rho(\vec{V} \cdot \vec{n}) ds = 0 \quad (4.4)$$

$$\int_r \rho \vec{F} d\tau - \int_s P \vec{n} ds - \int_s \rho(\vec{V} \cdot \vec{n}) \vec{V} ds = 0 \quad (4.5)$$

$$\int_s (P + \frac{1}{2} \rho V^2 - \rho g z)(\vec{V} \cdot \vec{n}) ds = 0 \quad (4.6)$$

For the two dimensional wave current interaction considered here and neglecting energy dissipation, these equations become simply

$$Q_{wo} + Q_{co} - Q_{wc} = 0 \quad (4.7)$$

$$M_{wo} + M_{co} - M_{wc} = 0 \quad (4.8)$$

$$E_{wo} + E_{co} - E_{wc} = 0 \quad (4.9)$$

where Q , M , E respectively represent the mean mass, momentum, and energy flux transfer across vertical planes normal to the x coordinate and of unit width. The subscripts "wo", "co" are used respectively to denote the current-free wave and wave-free current field quantities, and "wc" is used to denote a combined wave-current field quantity. All fluxes in equations (4.7), (4.8) and (4.9) have the same datum, the horizontal solid bed.

The three mean fluxes Q , M , E are given by the following equations

$$Q = \int_{-d}^{\eta} \rho u dz \quad (4.10)$$

$$M = \int_{-d}^{\eta} (\rho \dot{z} + \rho u^2) dz \quad (4.11)$$

$$E = \overline{\int_{-d}^{\eta} (P + \frac{1}{2}\rho(u^2 + w^2) + \rho gz)udz} \quad (4.12)$$

where u , w are the horizontal and vertical particle velocity respectively, P is the pressure, and the bar over the integration represents taking average over time.

4.2 Mean mass, momentum, energy fluxes

4.2.1 Fluxes in a current-free wave field

For the coordinate system with z vertically upwards from the undisturbed fluid surface, the second order potential function and surface profile of a current-free wave field are given by

$$\begin{aligned} \phi_{wo} = & \frac{a_0 \sigma_0}{K_0} \frac{\cosh K_0(z + d_0)}{\sinh K_0 d_0} \sin(K_0 x - \sigma_0 t) + \\ & + \frac{3}{8} a_0^2 \sigma_0 \frac{\cosh 2K_0(z + d_0)}{\sinh^4 K_0 d_0} \sin 2(K_0 x - \sigma_0 t) \end{aligned} \quad (4.13)$$

$$\begin{aligned} \eta_0 = & a_0 \cos(K_0 x - \sigma_0 t) + \\ & + \frac{1}{2} K_0 a_0^2 \left(1 + \frac{3}{2 \sinh^2 K_0 d_0} \right) \\ & \coth K_0 d_0 \cos 2(K_0 x - \sigma_0 t) \end{aligned} \quad (4.14)$$

The pressure to the second order is given as

$$P_{wo} = -\rho g z - \rho \frac{\partial \phi_{wo}}{\partial t} - \frac{1}{2} \rho \left[\left(\frac{\partial \phi_{wo}}{\partial x} \right)^2 + \left(\frac{\partial \phi_{wo}}{\partial z} \right)^2 \right] + \frac{1}{2} \rho g K_o a_o^2 \frac{1}{\sinh 2K_o d_o} \quad (4.15)$$

According to equations (4.10), (4.11), and (4.12), for the above wave field the mean mass, momentum, and energy flux could be obtained. They are in the form

$$Q_{wo} = \frac{1}{2\pi} \int_0^{2\pi} \int_{-d_o}^{\eta_o} \rho \frac{\partial \phi_{wo}}{\partial x} dz d\theta_o \quad (4.16)$$

$$M_{wo} = \frac{1}{2\pi} \int_0^{2\pi} \int_{-d_o}^{\eta_o} [P_{wo} + \rho \left(\frac{\partial \phi_{wo}}{\partial x} \right)^2] dz d\theta_o \quad (4.17)$$

$$E_{wo} = \frac{1}{2\pi} \int_0^{2\pi} \int_{-d_o}^{\eta_o} \left\{ P_{wo} + \frac{1}{2} \rho \left[\left(\frac{\partial \phi_{wo}}{\partial x} \right)^2 + \left(\frac{\partial \phi_{wo}}{\partial z} \right)^2 \right] + \rho g z \right\} dz d\theta_o \quad (4.18)$$

where $\theta_o = K_o x - \sigma_o t$

Now breaking the integration from $-d_o$ to η_o into an integration from $-d_o$ to 0 plus an integration from 0 to η_o and taking the following approximation

$$\int_0^{x_0} f(x) dx = x_0 f(0) + O(x_0^2) \quad (4.19)$$

when x_0 is relatively small, equations (4.16), (4.17), (4.18) become

$$Q_{w_0} = \frac{1}{2\pi} \int_0^{2\pi} \int_{-d}^0 \rho \frac{\partial \phi_{w_0}}{\partial x} dz d\theta_0 + \frac{1}{2\pi} \int_0^{2\pi} \rho \eta_0 \frac{\partial \phi_{w_0}}{\partial x}(x, 0, t) d\theta_0 \quad (4.20)$$

$$M_{w_0} = \frac{1}{2\pi} \int_0^{2\pi} \int_{-d}^0 [P_{w_0} + \rho \left(\frac{\partial \phi_{w_0}}{\partial x} \right)^2] dz d\theta_0 + \frac{1}{2\pi} \int_0^{2\pi} \eta_0 \{ P_{w_0}(x, 0, t) + \rho \left[\frac{\partial \phi_{w_0}}{\partial x}(x, 0, t) \right]^2 \} d\theta_0 \quad (4.21)$$

$$E_{w_0} = \frac{1}{2\pi} \int_0^{2\pi} \int_{-d}^0 \{ P_{w_0} + \frac{1}{2} \rho \left[\left(\frac{\partial \phi_{w_0}}{\partial x} \right)^2 + \left(\frac{\partial \phi_{w_0}}{\partial z} \right)^2 \right] + \rho g z \} \frac{\partial \phi_{w_0}}{\partial x} dz d\theta_0 + \frac{1}{2\pi} \int_0^{2\pi} \eta_0 \{ P_{w_0}(x, 0, t) + \frac{1}{2} \rho \left[\left(\frac{\partial \phi_{w_0}}{\partial x}(x, 0, t) \right)^2 + \left(\frac{\partial \phi_{w_0}}{\partial z}(x, 0, t) \right)^2 \right] \} \frac{\partial \phi_{w_0}}{\partial x}(x, 0, t) d\theta_0 \quad (4.22)$$

Substituting P_{w_0} , ϕ_{w_0} , and η_0 into the above equations and performing the integrations yields, to $O(Ka_0^2)$

$$Q_{wo} = \frac{1}{2} \rho a_o^2 K_o \sqrt{\frac{g}{K_o} \coth K_o d_o} \quad (4.23)$$

$$M_{wo} = \frac{1}{2} \rho g a_o^2 \left(\frac{1}{2} + \frac{2K_o d_o}{\sinh 2K_o d_o} \right) + \frac{1}{2} \rho g d_o^2 \quad (4.24)$$

$$E_{wo} = \frac{1}{4} \rho g a_o^2 \frac{\sigma_o}{k_o} \left(1 + \frac{2K_o d_o}{\sinh 2K_o d_o} \right) \quad (4.25)$$

4.2.2 Fluxes in a wave-free current field

The potential function of a wave-free uniform irrotational current field is given by

$$\phi_{co} = U_o x \quad (4.26)$$

for some uniform stream U_o .

The pressure distribution along a vertical section is

$$P_c = -\rho g z \quad (4.27)$$

On using equations (4.10), (4.11), and (4.12), the mean mass, momentum, and energy fluxes in a wave-free current field are then

$$Q_{co} = \int_{-d}^0 \rho \frac{\partial \phi_{co}}{\partial x} dz \quad (4.28)$$

$$M_{co} = \int_{-d}^0 \rho \left(\frac{\partial \phi_{co}}{\partial x} \right)^2 dz \quad (4.29)$$

$$E_{co} = \int_{-d}^0 \left[P_{co} + \frac{1}{2} \rho \left(\frac{\partial \phi_{co}}{\partial x} \right)^2 + \rho g z \right] \frac{\partial \phi_{co}}{\partial x} dz \quad (4.30)$$

Performing the integration gives

$$Q_{co} = \rho d_o U_o \quad (4.31)$$

$$M_{co} = \rho d_o U_o^2 \quad (4.32)$$

$$E_{co} = \frac{1}{2} \rho d_o U_o^3 \quad (4.33)$$

4.2.3 Fluxes in a wave-current field

For the combined wave-current field the three mean fluxes across an arbitrary vertical plane in the flow of unit width can be expressed as

$$Q_{wc} = \frac{1}{2\pi} \int_0^{2\pi} \int_{-d}^d \rho \frac{\partial \Phi}{\partial x} dz d\theta \quad (4.34)$$

$$M_{wc} = \frac{1}{2\pi} \int_0^{2\pi} \int_{-d}^d [P + \rho \left(\frac{\partial \Phi}{\partial x}\right)^2] dz d\theta \quad (4.35)$$

$$E_{wc} = \frac{1}{2\pi} \int_0^{2\pi} \int_{-d}^d \left\{ P + \frac{1}{2} \rho \left[\left(\frac{\partial \Phi}{\partial x}\right)^2 + \left(\frac{\partial \Phi}{\partial z}\right)^2 \right] + \rho g z \right\} \frac{\partial \Phi}{\partial x} dz d\theta \quad (4.36)$$

where $\theta = Kx - \sigma t$

Using the approximation expressed in equation (4.19), Q_{wc} , M_{wc} and E_{wc} could be written as

$$Q_{wc} = \frac{1}{2\pi} \int_0^{2\pi} \int_{-d}^d \rho \frac{\partial \Phi}{\partial x} dz d\theta + \frac{1}{2\pi} \int_0^{2\pi} \eta \rho \frac{\partial \Phi}{\partial x}(x, 0, t) d\theta \quad (4.37)$$

$$M_{wc} = \frac{1}{2\pi} \int_0^{2\pi} \int_{-d}^d [P + \rho \left(\frac{\partial \Phi}{\partial x}\right)^2] dz d\theta + \frac{1}{2\pi} \int_0^{2\pi} \eta \{ P(x, 0, t) + \rho \left[\frac{\partial \Phi}{\partial x}(x, 0, t) \right]^2 \} d\theta \quad (4.38)$$

$$\begin{aligned}
E_{wc} = & \frac{1}{2\pi} \int_0^{2\pi} \int_{-d}^0 \left\{ P + \frac{1}{2} \rho \left[\left(\frac{\partial \Phi}{\partial x} \right)^2 + \right. \right. \\
& \left. \left. + \left(\frac{\partial \Phi}{\partial z} \right)^2 \right] + \rho g z \right\} \frac{\partial \Phi}{\partial x} dz d\theta + \\
& + \frac{1}{2\pi} \int_0^{2\pi} \eta \left\{ P(x, 0, t) + \frac{1}{2} \left[\left(\frac{\partial \Phi}{\partial x}(x, 0, t) \right)^2 + \right. \right. \\
& \left. \left. + \left(\frac{\partial \Phi}{\partial z}(x, 0, t) \right)^2 \right] \right\} \frac{\partial \Phi}{\partial x}(x, 0, t) dz d\theta
\end{aligned} \tag{4.39}$$

The fluxes of the combined wave-current field can be obtained to order Ka^2 on substituting Φ , P and η from equations (3.61), (3.73), (3.63) into equation (4.37), (4.38), (4.39). Performing the integrations gives to $O(Ka^2)$

$$Q_{wc} = \rho dU + \frac{1}{2} \rho a^2 K \sqrt{\frac{g}{K} \coth Kd} \tag{4.40}$$

$$\begin{aligned}
M_{wc} = & \rho dU^2 + \frac{1}{2} \rho g d^2 + \frac{1}{2} \rho g a^2 \left(\frac{1}{2} + \frac{2Kd}{\sinh 2Kd} \right) + \\
& + \rho K U a^2 \sqrt{\frac{g}{K} \coth Kd}
\end{aligned} \tag{4.41}$$

$$\begin{aligned}
E_{wc} = & \frac{1}{2} \rho dU^3 + \\
& + \frac{1}{4} \rho g a^2 \sqrt{\frac{g}{K} \tanh Kd} \left(1 + \frac{2Kd}{\sinh 2Kd} \right) + \\
& + \frac{3}{4} \rho a^2 U^2 K \sqrt{\frac{g}{K} \coth Kd} + \\
& + \frac{1}{4} \rho g a^2 U \left(3 + \frac{4Kd}{\sinh 2Kd} \right)
\end{aligned} \tag{4.42}$$

E_{wc} as expressed by equation (4.42) is easily recognized to be R_x in equation (35) of Longuet-Higgins and Stewart (1960). The four terms in equation (4.42) above are identically equal to their R_0, R_1, R_2, R_3 respectively. Moreover, E_{wc} could be easily written as the following sum:

$$E_{wc} = E_w C_{gr} + (E_w + S_z)U + E_U u_d + e_w U + E_U U \quad (4.43)$$

where

$$E_w = \frac{1}{2} \rho g a^2 \quad (4.44)$$

denotes the mean wave energy density per unit horizontal area in the absence of a stream;

$$C_{gr} = \frac{d\sigma_r}{dK} = \frac{1}{2} \left(1 + \frac{2Kd}{\sinh 2Kd} \right) C_r \quad (4.45)$$

denotes the group velocity relative to still water;

$$S_z = \frac{1}{4} \rho g a^2 \left(1 + \frac{4Kd}{\sinh 2Kd} \right) \quad (4.46)$$

denotes the radiation stress as defined in Longuet-Higgins and Stewart (1960);

$$E_U = \frac{1}{2} \rho d U^2 \quad (4.47)$$

denotes the mean current energy density in the absence of the wave;

$$u_d = \frac{1}{2} \frac{a^2 g}{C_r d} \quad (4.48)$$

denotes the relative wave drift velocity; and

$$e_w = \frac{1}{2} \rho \frac{g a^2}{\sigma_r} K U \quad (4.49)$$

with $\rho g a^2 / (2\sigma_r)$ representing the so called wave action (Crapper 1984).

A discussion on the physical meaning of each term in equation (4.42) and the radiation stress, as well as the energy transfer in the combined wave current field is given in appendix A of this thesis.

4.3 Relationships between L , H , d , U and L_o , H_o , d_o , U_o

By substituting the expressions for Q_{co} , M_{co} , E_{co} , Q_{wo} , M_{wo} , E_{wo} , Q_{wc} , M_{wc} , E_{wc} from equations (4.23), (4.24), (4.25), (4.31), (4.32), (4.33), (4.40), (4.41), (4.42) into equations (4.7), (4.8) and (4.9) and combining the dispersion relation, equations (3.64) and (3.65), of the combined wave-current field, the relationships between L , H , d , U and L_o , H_o , d_o , U_o are established by the following system of nonlinear equations

$$\frac{\sigma}{K} = U + \sqrt{\frac{g}{K} \tanh Kd}; \quad (4.50)$$

$$\begin{aligned} \rho d_o U_o + \frac{1}{2} \rho a_o^2 \sqrt{K_o g \coth K_o d_o} &= \\ = \rho d U + \frac{1}{2} \rho a^2 \sqrt{K g \coth K d}; \end{aligned} \quad (4.51)$$

$$\begin{aligned} \rho d_o U_o^2 + \frac{1}{2} \rho g d_o^2 + \frac{1}{2} \rho g a_o^2 \left(\frac{1}{2} + \frac{2K_o d_o}{\sinh 2K_o d_o} \right) &= \\ = \rho d U^2 + \frac{1}{2} \rho g d^2 + \frac{1}{2} \rho g a^2 \left(\frac{1}{2} + \frac{2Kd}{\sinh 2Kd} \right) + \\ + \rho K U a^2 \sqrt{\frac{g}{K} \coth Kd}; \end{aligned} \quad (4.52)$$

$$\begin{aligned} \frac{1}{2} \rho d_o U_o^3 + \frac{1}{4} \rho g a_o^2 \frac{\sigma}{K_o} \left(1 + \frac{2K_o d_o}{\sinh 2K_o d_o} \right) &= \\ = \frac{1}{2} \rho d U^3 + \frac{1}{4} \rho g a^2 \sqrt{\frac{g}{K} \tanh Kd} \left(1 + \frac{2Kd}{\sinh 2Kd} \right) + \\ + \frac{3}{4} \rho K U^2 a^2 \sqrt{\frac{g}{K} \coth Kd} + \\ + \frac{1}{4} \rho U a^2 g \left(3 + \frac{4Kd}{\sinh 2Kd} \right); \end{aligned} \quad (4.53)$$

Now, the following non dimensional variables are introduced;

$$A = \frac{a_o^2}{d_o^2} = \frac{H_o^2}{4d_o^2}; \quad (4.54)$$

$$B = \frac{U_o}{C_o}; \quad (4.55)$$

$$D = \frac{L_o}{d_o}; \quad (4.56)$$

$$\bar{W} = \frac{d}{d_o}; \quad (4.57)$$

$$X = \frac{U}{C_o}; \quad (4.58)$$

$$Y = \left(\frac{L}{L_o}\right)^{1/2}; \quad (4.59)$$

and

$$Z = \frac{a^2}{d_o^2} = \frac{H^2}{4d_o^2}; \quad (4.60)$$

In terms of the above variables the system of equations (4.50), (4.51), (4.52), (4.53) becomes

$$Y^2 = X + Y \sqrt{\coth \frac{2\pi}{D} \tanh \frac{2\pi W}{DY^2}}; \quad (4.61)$$

$$\begin{aligned} BD + \pi A \coth \frac{2\pi}{D} &= \\ &= DWX + \pi Z \frac{1}{Y} \sqrt{\coth \frac{2\pi}{D} \coth \frac{2\pi W}{DY^2}}; \end{aligned} \quad (4.62)$$

$$\begin{aligned} 1 + A \left(\frac{1}{2} + \frac{2\pi}{D} \frac{1}{\sinh \frac{2\pi}{D} \cosh \frac{2\pi}{D}} \right) + \frac{D}{\pi} B^2 \tanh \frac{2\pi}{D} &= \\ = W^2 + Z \left(\frac{1}{2} + \frac{2\pi W}{DY^2} \frac{1}{\sinh \frac{2\pi W}{DY^2} \cosh \frac{2\pi W}{DY^2}} \right) + \\ + \frac{D}{\pi} X^2 W \tanh \frac{2\pi}{d} + \frac{2XZ}{Y} \sqrt{\tanh \frac{2\pi}{D} \coth \frac{2\pi W}{DY^2}}; \end{aligned} \quad (4.63)$$

$$\begin{aligned} \frac{D}{\pi} B^3 \tanh \frac{2\pi}{D} + A \left(1 + \frac{2\pi}{D} \frac{1}{\sinh \frac{2\pi}{D} \cosh \frac{2\pi}{D}} \right) &= \\ = \frac{D}{\pi} W X^3 \tanh \frac{2\pi}{D} + 3Z X^2 \frac{1}{Y} \sqrt{\tanh \frac{2\pi}{D} \coth \frac{2\pi W}{DY^2}} + \\ + ZY \sqrt{\coth \frac{2\pi}{D} \tanh \frac{2\pi W}{DY^2}} \left(1 + \frac{2\pi W}{DY^2} \frac{1}{\sinh \frac{2\pi W}{DY^2} \cosh \frac{2\pi W}{DY^2}} \right) + \\ + ZX \left(3 + \frac{4\pi W}{DY^2} \frac{1}{\sinh \frac{2\pi W}{DY^2} \cosh \frac{2\pi W}{DY^2}} \right) \end{aligned} \quad (4.64)$$

The set of equations (4.61), (4.62), (4.63), and (4.64) establishes the relationship between the current-free wave, and wave-free current and the corresponding combined wave-current field. Given the current-free wave height H_0 , length L_0 , wave-free current speed U_0 and water depth d_0 , A , B , D could be determined by using equations (4.54), (4.55), (4.56). The variables W , X , Y , and Z can then be computed by solving numerically the above algebraic equations. The wave height, length, current speed and mean water depth of the combined wave-current field are then obtained as

$$H = 2D_0\sqrt{Z} \quad (4.65)$$

$$L = L_0Y^2 \quad (4.66)$$

$$U = C_0X \quad (4.67)$$

and

$$d = d_0W. \quad (4.68)$$

In equation (4.50) or its nondimensional equivalent equation (4.61) the positive root is adopted. However, the value of the square root in (4.50) is taken as positive when considering the interaction of wave with a following current and negative when considering an opposing current. In this fashion all possible distinct solutions, as described for example in Peregrine (1970) could be taken into account. Once the values of the wave-current field

parameters in equations (4.61) - (4.64) are obtained, one of the four solutions could then be identified a posteriori, according to the following classification:

$$(i) \quad U > 0 \quad (4.69)$$

$$(ii) \quad -C_{gr} < U < 0 \quad (4.70)$$

$$(iii) \quad -C_r < U < -C_{gr} \quad (4.71)$$

$$(iv) \quad U < -C_r \quad (4.72)$$

where C_{gr} is given by equation (4.45).

Cases (i) and (ii) are of engineering interest. Cases (iii) and (iv) are possible solutions when waves interact with an opposing current. Discussion of their physical interpretation is given in Longuet-Higgins and Stewart (1960) or Sarpkaya and Isaacson (1980). To be noted however, that in an opposing current the present theory, could fail for relatively small negative ratios of U_0/C_0 because of the increase in this case of the predicted height H of the surface disturbance of the combined wave-current field.

4.4 Computational considerations and results

The set of nonlinear equations (4.61) — (4.64) is solved numerically for W , X , Y , and Z , using a Newton technique. It is worth noting the convergence and stability behavior of the iteration. For a given wave data H_o , L_o , d_o and current velocity U_o , the solution is found for any set of arbitrary initial guess values for H , L , d , and U . The wave before the interaction and the combined wave-current after the interaction should both satisfy the assumptions of the second order approximation. It seems that general sufficient conditions for the uniqueness of the solution of the nonlinear system of equations (4.61) — (4.64) for a given ratio U_o/C_o , are not available. However, the range of values chosen for the parameters in this study, produced the only solutions presented herein. In the present solution, a negative value for U_o represents a current flowing in the opposite direction of the wave propagation.

As an example the plane wave defined by the parameters $H_o = 1.5m$, $L_o = 100.0m$ on still water of depth $d_o = 25.0m$ is considered to interact with uniform streams of current ratios U_o/C_o varying over the range of values between -0.20 to $+0.20$. The wave length, wave height, current speed and the water depth of the wave-current field are found on solving the system (4.61) — (4.64). The wave length ratio L/L_o , wave height ratio H/H_o , current change ratio $\Delta U/C_o$ and depth change ratio $\Delta d/d_o$, where

$\Delta U = U - U_0$ denotes the variation in U and $\Delta d = d - d_0$ denotes the variation in depth, are easily evaluated. These quantities are respectively plotted in figures (4.1), (4.2), (4.3) and (4.4) against U_0/C_0 .

As expected, the length of the wave on the surface of the combined field decreases when the wave train encounters an opposing current, while increasing when the current U_0 is in the same direction, see figure (4.1). Also, not surprisingly, a reverse behavior is noticed in the height of the wave, see figure (4.2), increasing in magnitude in an opposing current and decreasing when meeting with a following current. Qualitatively these results compare favourably with a number of other researchers' findings, for example Brevik and Aas (1980), Longuet-Higgins and Stewart (1960), Jonsson, Skougaard and Wang (1970) and Thomas (1981). However, quantitatively it would be difficult to make any comparison with other theoretical results, since the present approach is a departure from other investigations in that it does not include a known, a priori, upwelling or horizontal inflow from the sides, nor does it assume a given change in the bottom configuration. However, a comparison with the experimental results obtained by Thomas (1981) has been done, and will be presented in the following chapter.

The change in the mean value of the current is presented in figure (4.3) as $(U - U_0)/C_0$. It shows an increase in the magnitude of the average stream velocity U of the combined field over the wave-free current U_0 when

the wave and current propagate in the same direction and a decrease otherwise. The relative change in the mean water depth due to the wave-current interaction is given in figure (4.4) as $(d - d_0)/d_0$. This figure shows a decrease in the mean value of the wave-current field depth d relative to d_0 , when the wave and current propagate in the same direction. An increase is noticed otherwise. Both changes are relatively small quantities and depend on the initial velocity ratio U_0/C_0 .

It is noted that the herein developed solution set of the nonlinear system is found to be independent of the initial guess used in conjunction with Newton's iteration technique and the considered range of values of U_0/C_0 . However there is no point in graphing the relations beyond the value of $U_0/C_0 = -0.16$ since the second order wave theory will then fail for this example, due to the increase in wave height and decrease in wave length. A negative value given to the ratio U_0/C_0 represents a current in the direction opposite that of wave propagation. For the considered range of values i.e. for $-0.16 < U_0/C_0 < 0$ it is easy to find that the corresponding range of U is such that $-C_{gr} < U < 0$ with C_{gr} given by equation (4.45).

For completeness numerical values for the ratios L/L_0 , H/H_0 , $\Delta U/C_0$, and $\Delta d/d_0$ are given for a range of values of the ratio U_0/C_0 of the wave-free current to the current-free wave celerity and are tabulated in table (C.1), (C.2), (C.3), and (C.4) in the Appendix 4. Tables (C.1) and (C.2) give the wave height and wave length ratios respectively. Table (C.3) gives the

current variation ratio $(U - U_0)/C_0$, while table (C.4) displays the depth variation ratio $(d - d_0)/d_0$. It is found that the changes in the mean depth and the mean current are very much less pronounced in comparison to the changes in wave height and wave length. Table (C.3) shows that the mean value of the current term in the combined field increases in a following wave and decreases when flowing in an opposite direction to the wave propagation. Table (C.4) on the other hand, shows that the depth of the combined wave-current field changes also slightly from its value d_0 .

The values in the four tables presented in appendix C are within the preassigned convergence criterion chosen in conjunction with the numerical iteration used and within the precision kept for all variables. The accuracy of the results is checked in an ad hoc fashion, on running the computer program several times using different precision in the computer calculations. Four-time precision, i.e. typically 24 decimal digits is the degree of precision used for all variables in the computation.

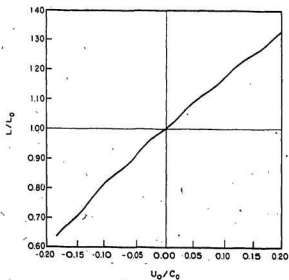


Fig. 4.1 Wave length ratio L/L_0 vs current speed ratio U_0/C_0 for plane wave parameters $a_s = 0.75$ m, $L_s = 100.0$ m, $d_s = 25.0$ m.

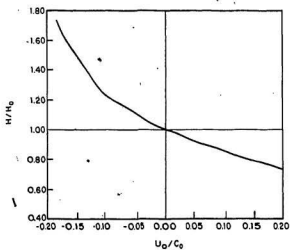


Fig. 4.2 Wave height ratio H/H_0 vs current ratio U_0/C_0 for plane wave parameters $a_s = 0.75$ m, $L_s = 100.0$ m, $d_s = 25.0$ m.

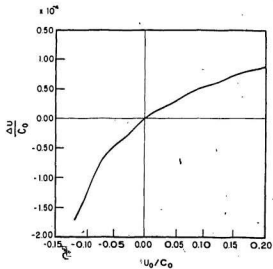


Fig. 43 Current change ratio $(U - U_0)/C_0$ vs current ratio U_0/C_0 , for plane wave parameters $a_s = 0.75$ m, $L_s = 100.0$ m, $d_s = 25.0$ m.

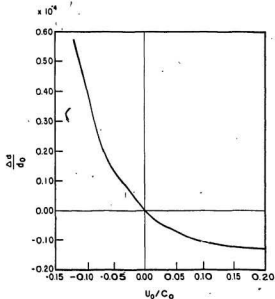


Fig. 44 Depth change $(d - d_0)/d_0$ vs current ratio U_0/C_0 , for plane wave parameters $a_s = 0.75$ m, $L_s = 100.0$ m, $d_s = 25.0$ m.

Chapter 5

Prediction of the Combined Wave-Current Field Properties

In chapter 2 the properties of the combined wave-current motion have been given in terms of wave height H , length L , current speed U and the water depth d of the combined wave-current field. In chapter 3 the relation between the wave height H , length L , current speed U , water depth d of the combined wave-current field and the current-free wave height H_0 , wave length L_0 , wave-free current speed U_0 , water depth d_0 has been established, so that H , L , U , and d could be calculated when H_0 , L_0 , U_0 , and d_0 are given. These allow one to predict the properties, such as particle velocity, acceleration, pressure distributions etc., of the combined wave-current field by using the current-free wave height H_0 , length L_0 , wave-free current speed U_0 , and water depth d_0 .

The procedure involves the following steps. 1). Using the method given in chapter 4 to calculate numerically H , L , U , and d ; 2). Using H , L , U , and d and the equations in chapter 3 to calculate the particle velocity, acceleration, pressure distribution etc. of the combined wave-current field.

Considering the same example used in chapter 4, i.e. considering a current-free wave with $H_0 = 1.5$ m, $L_0 = 100.0$ m, on water of depth $d_0 = 25$ m, the maximum particle velocity distribution along the water depth for $U_0/C_0 = -0.15$, $U_0/C_0 = -0.10$, $U_0/C_0 = -0.05$, $U_0/C_0 = 0.0$, $U_0/C_0 = 0.05$, $U_0/C_0 = 0.10$, and $U_0/C_0 = 0.15$ are plotted in figures (5.1)—(5.7) against z/d . In the figures the solid line represents the amplitude of the horizontal particle velocity and the broken line represents the amplitude of the vertical particle velocity. The corresponding maximum particle acceleration are plotted in figures (5.8)—(5.14) respectively. The solid line represents the distribution of the horizontal particle acceleration. The broken line shows the vertical particle acceleration along z/d . Figures (5.15)—(5.18) give the trajectory of a particle at the point (0,-5) in the combined wave-current field for the values $U_0/C_0 = -0.01$, $U_0/C_0 = -0.02$, $U_0/C_0 = 0.01$, and $U_0/C_0 = 0.02$ respectively.

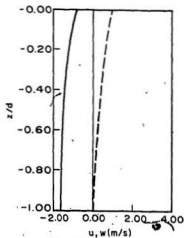


Fig. 5.1 $U_0/C_0 = -0.15$

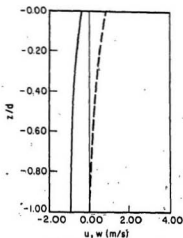


Fig. 5.2 $U_0/C_0 = -0.10$

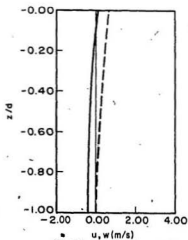


Fig. 5.3 $U_0/C_0 = -0.05$

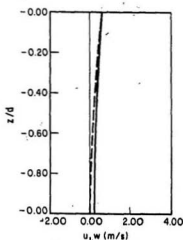
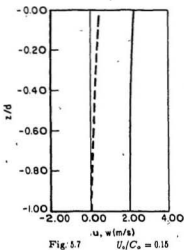
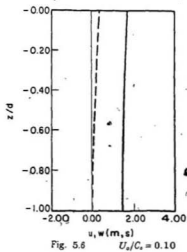
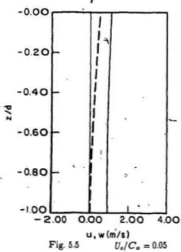


Fig. 5.4 $U_0/C_0 = 0.00$

Maximum particle velocity distribution along water depth

(— Horizontal ; ... Vertical)



Maximum particle velocity distribution along water depth

(— Horizontal ; - - - Vertical)

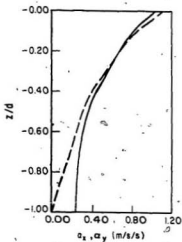


Fig. 5.8 $U_s/C_s = -0.15$

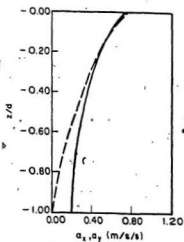


Fig. 5.9 $U_s/C_s = -0.70$

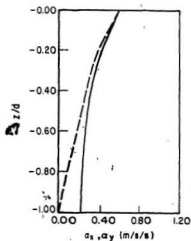


Fig. 5.10 $U_s/C_s = -0.05$

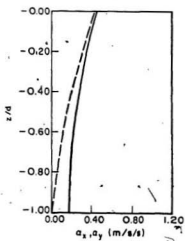


Fig. 5.11 $U_s/C_s = 0.00$

Maximum particle acceleration distribution along water depth
 (— Horizontal : - - Vertical)

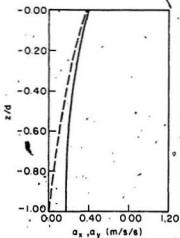


Fig. 5.12 $U_0/C_0 = 0.05$

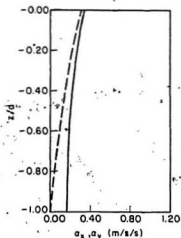


Fig. 5.13 $U_0/C_0 = 0.10$

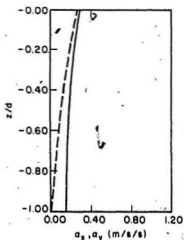


Fig. 5.14 $U_0/C_0 = 0.15$

Maximum particle acceleration distribution along water depth

(— Horizontal ; - - - Vertical)

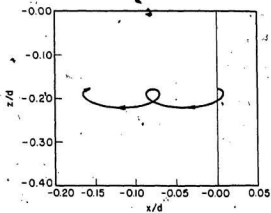


Fig. 5.15 $U_s/C_0 = -0.02$

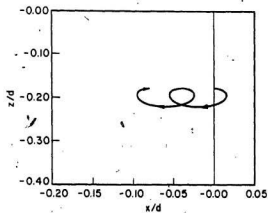


Fig. 5.16 $U_s/C_0 = -0.01$

Trajectories of particle at $z/d = -0.2$ in the
wave-current field

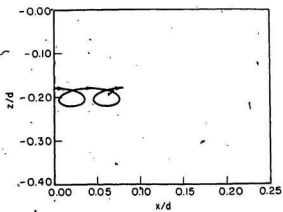


Fig. 5.17 $U_0/C_0 = 0.01$

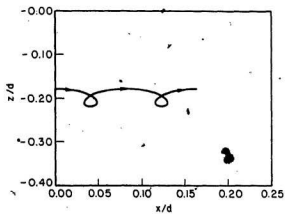


Fig. 5.18 $U_0/C_0 = 0.02$

Trajectories of particle at $z/d = -0.2$ in the
wave-current field

Chapter 6

Comparison Between Present Theory and Experiment

The experimental results cited here were published by G. P. Thomas (1981) in *Journal of Fluid Mechanics*. His experimental programme was carried out at the Hydraulic Laboratory of the Department of Civil Engineering, University of Bristol. A longitudinal schematic section of the flume used for the experiments is shown Figure (6.1).

The flume used in the experiment had an overall length of approximately 27 m. The working section between the beach and the paddle had a uniform width of 0.72 m and a horizontal floor. Behind the beach the flume width was approximately twice that of the working section, and was so designed to set as a stilling basin which minimized fluctuations introduced by the pump when currents were used.

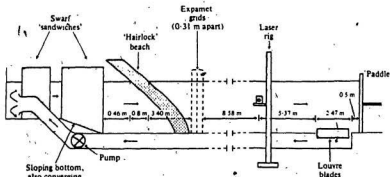


Fig. 6.1 Schematic section of the wind-wave-current flume in the Hydraulics Laboratory, Department of Civil Engineering, University of Bristol. The drawing is not to scale and does not show the wind facility Thomas 1981.

Waves were generated by a hydraulically driven flat paddle board which could be controlled by either a regular signal generator or a pre-recorded random signal as required. Unwanted wave reflection were removed by a beach constructed of three thicknesses of 'Hairlock' bound in an 'expamet' sandwich. The wave reflection coefficient, which is defined as the ratio of the reflected wave height to the incident wave height, for waves was reported to be less than 2 percent (Thomas, 1981).

The current motion was driven by a pump with an adjustable motor and provides a re-circulatory flow in which the current in the flume is adverse to the direction of the wave propagation. Water was removed from the flume over a distance of approximately 2.5 m in front of the paddle and travelled via a return duct under the main floor of the flume, to be pumped into the stilling basin behind the beach (Thomas, 1981).

The wave and the current velocities were measured using Laser-Doppler anemometry (LDA). The laser was a Spectra-Physics 12A (15mw) and the transmitting receiving and processing optical units were contained in a modified Mark 1 DISA system. Wave heights and profiles were measured using resistance type gauges built to the design developed at the Hydraulics Research Station, Wallingford. The oscillatory LDA and wave probe output was analysed on-line by a S.E. Laser model SM2002A Transfer Function Analyser, which was also used to generate the regular sinusoidal waves. The non-oscillatory LDA output, corresponding to the mean current, was evaluated using an averaging microprocessor voltmeter (Thomas, 1981).

The experimental data were given as follows. For still water depth $d_o = 0.57$ m, current-free wave length $L_o = 2.261$ m, current-free wave amplitude $a_o = 9.18$ mm, which gives the wave velocity of $C_o = 1.8014$ m/s, the measurements were carried out for four estimated mean current speeds, namely $U_o = -59.7$ mm/s; -116.2 mm/s; -159.8 mm/s, -203.0 mm/s. The minus sign means the current is adverse to the direction of the wave propagation.

Changes in wave length and in wave amplitude and the horizontal particle velocity component distribution of the wave after the interaction were measured. Although the water depth change was not measured, the phenomenon was noticed and reported by Thomas, and referred to as set-up or set-down.

The measured wave length and amplitude changes in the ratios of a/a_0 and L/L_0 by Thomas (1981) and the predicted values by the present theory are listed in Table (6.1) and Table (6.2), and plotted in Figure (6.2) and Figure (6.3) respectively. Comparison of the measured (by G.P. Thomas 1981) and the predicted (by the present method) wave amplitude and length changes shows good agreement between the two data. The maximum difference between the predicted and the measured values is less than 3.6% in amplitude and 3.0% in length. Also to be noted that this difference is not uniform over the values tested. These results could be considered surprisingly accurate.

The present method also predicts the changes in the current velocity U_0 and the water depth d_0 . These are presented in nondimensional form in Table (6.3) for completeness. These changes in the current and in the water depth were neglected by other theories.

Table (6.3) shows that the method presented in this thesis predicts an increase in the water depth and decrease in the mean current velocity when waves interact with an adverse current over a horizontal bed.

The measured amplitudes of wave like horizontal particle velocities (Thomas 1981) in the wave-current field and corresponding theoretical predictions using the present theory are presented graphically in Figures (6.4)—(6.7) for the current values U_0 specified in Thomas (1981). In each of the figures the experimental results of Thomas are shown by a circle and

a predicted profile using the present approach by a solid line. Very good agreement is generally seen to exist between the measured (Thomas 1981) and predicted (present theory) velocities. The mean discrepancy between the theoretical and the measured velocity data is of the order of 4%. It should be noted that the method presented in this thesis could be used for second order wave and current interaction predictions, but no experimental results are available for comparison.

U_o	U_o/C_o	measured Thomas (1981) L/L_o	predicted present method L/L_o	diff. %
0.0	0.0000	1.0000	1.000	0.00%
-59.7	-0.0332	0.954	0.940	1.47%
-116.2	-0.0645	0.894	0.882	1.34%
-159.8	-0.0888	0.844	0.835	1.07%
-203.0	-0.1127	0.810	0.786	2.96%

Table 6.1 Comparison between the measured and the predicted wave length changes.

U_o	U_o/C_o	measured Thomas (1981) a/a_o	predicted present method a/a_o	diff. %
0.0	0.0000	1.000	1.000	0.00%
-59.7	-0.0332	1.085	1.068	1.57%
-116.2	-0.0645	1.156	1.147	0.78%
-159.8	-0.0888	1.267	1.222	3.55%
-203.0	-0.1127	1.309	1.315	0.46%

Table 6.2 Comparison between the measured and the predicted wave height changes.

U_o (mm/s)	U_o/C_o	$\Delta d/d_o$	$\Delta U/C_o$
-59.7	-0.0332	0.040×10^{-4}	-0.386×10^{-4}
-116.2	-0.0645	0.111×10^{-4}	-0.877×10^{-4}
-159.8	-0.0888	0.203×10^{-4}	-1.395×10^{-4}
-203.0	-0.1127	0.342×10^{-4}	-2.095×10^{-4}

Table (6.3) Predicted values of $\Delta d/d_o$ and $\Delta U/C_o$, using the present method, where $\Delta d = |d - d_o|$ and $\Delta U = |U - U_o|$.

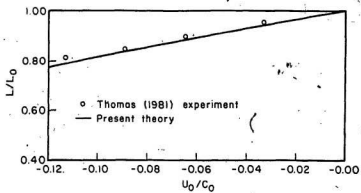


Fig. 6.2 Comparison between the present theoretical predictions and Thomas experimental results for wave length changes

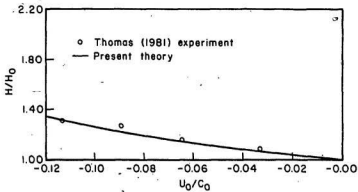


Fig. 6.3 Comparison between the present theoretical predictions and Thomas experimental results for wave height changes

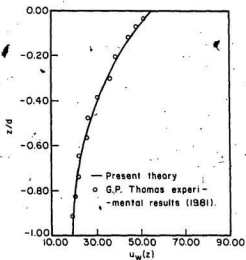


Fig. 6.4 $U_0 = -59.7$ mm/s

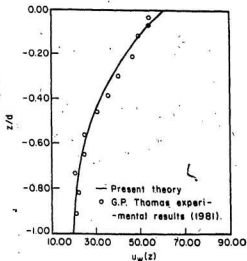


Fig. 6.5 $U_0 = -116.2$ mm/s

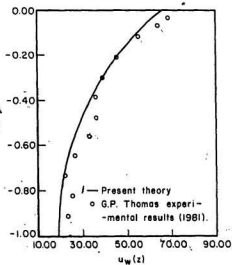


Fig. 6.6 $U_0 = -159.8$ mm/s

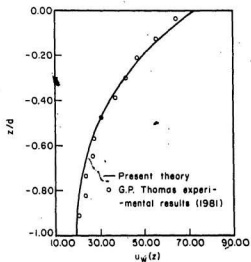


Fig. 6.7 $U_0 = -203.0$ mm/s

Comparison between the present theoretical predictions and Thomas experimental results on the wavelike horizontal particle velocity distribution along water depth.

Chapter 7

Conclusions and Recommendations for Further Research

The interaction of following or opposing uniform current and finite amplitude regular surface gravity waves of permanent form were studied. The combined wave-current field, resulting from the interaction of waves and a uniform current, was described by the velocity potential Φ , free surface profile η and the dispersion relation on the free surface, in terms of H , L , d , and U . The values of H , L , d , and U were computed from H_0 , L_0 , d_0 , and U_0 on solving a set of nonlinear equations obtained on satisfying the dispersion relation on the free surface and the conservation of mean mass, momentum and energy transfer to second order. Nonlinear wave-current interaction effects were taken into account. Apart from the usual, expected changes in the wave height and length it was found that the mean value of the current and water depth, also undergo changes which were computed

samepage in some numerical examples. Furthermore, the computed results on the changes in wave height and wave length were found to be more accurate by considering the changes in the current and the water depth. Comparison shows that the predicted values and the experimental results are in good agreement both in the changes of wave height, wave length and the properties of the combined wave-current field.

The prediction of waves and current interaction and combined wave-current field effects on engineering structures is an area of research that needs further work in order that the data and results may be supplied to the engineer responsible for loads estimation and design.

Currents that vary linearly or bilinearly with the depth were considered in the past and some attempts (See Dalrymple 1973) were made for modelling the interaction of waves with nonlinear current velocities. The effects of waves on nonlinear current distributions and on structures if any, need to be evaluated and verified in laboratory settings. In this context refraction and diffraction effects for small amplitude and finite amplitude waves in shear currents are also research area of interest.

References

- ARTHUR, R. S. (1950). Refraction of shallow water waves: the combined effect of currents and underwater topography. *Trans. Amer. Geophys. Union* 31, 549—552.
- BADDOUR, R. E. and SONG, S. W. (1987). On wave-current-structure interaction. *21st Annual Congress Canadian Meteorological and Oceanographic Society*. P. 45.
- BADDOUR, R. E. and SONG, S. W. (1988a). Water wave and current interaction. *Proc. 9th Symp. on Eng. Appl. of Mech.* 442 — 453.
- BADDOUR, R. E. and SONG, S. W. (1988b). On a rotational wave-current fluid flow. *Fluid Dynamics Internal Report, Fac. of Eng., M.U.N.*
- BRETHERTON, F. P. and GARRETT, C. J. R. (1968). Wavetrains in inhomogeneous moving media. *Proc. Roy. Soc., Ser. A* 302, 529—554.
- BREVIK, I. and AAS, B. (1980). Flume experiment on waves and currents I. Rippled bed. *Coastal Eng.* 3, 149—177.
- BREVIK, I. and AAS, B. (1980). Flume experiment on waves and currents II. Smooth bed. *Coastal Eng.* 4, 89—110.
- CRAIK, A. D. D. (1985). Wave interaction of fluid flows. *Camb. Univ. Press, Cambridge*.
- CRAPPER, G. D. (1984). Introduction to Water Waves. *John Wiley and Sons Inc. N. Y.*
- DALRYMPLE, R. A. (1973). Water wave models and wave forces with shear currents. *Technical Rep. No. 20 Coastal Oceanography Eng. Lab. Univ. of Florida, Gainesville, Florida*.
- DALRYMPLE, R. A. and DEAN, R. G. (1975). Waves of maximum height on uniform current. *J. of Waterways, Harbors, and Coastal Eng. Division* 101, No. 3, 259—268.
- DENNIS, H. (1973). Non-linear gravity-capillary surface waves in a slowly varying current. *J. Fluid Mech.* 57, Part 4, 797—802.

FREEMAN, N. C. and JOHNSON, R. S. (1970). Shallow water waves on shear flows. *J. Fluid Mech.* 42, 401-409.

HASSELMANN, K. (1971). On the mass and momentum transfer between short gravity waves and large-scale motions. *J. Fluid Mech.* 50, 189-205.

HUANG, N. E., CHEN, D. T., TUNG, C. C. and SMITH, J. R. (1972). Interactions between steady non-uniform currents and gravity waves with applications for measurements. *J. Phys Oceanogr.* 2, 420-431.

HUGHES, B. A. and STEWART, R. W. (1961). Interaction between gravity waves and a shear flow. *J. Fluid Mech.* 10, 385-400.

JOHNSON, J. W. (1947). The refraction of surface waves by currents. *Trans. Amer. Geophys. Union.* 28, 867-874.

JONSSON, I. G. (1978). Energy flux and wave action in gravity waves propagating on a current. *J. Hydr. Res.* 16, 223-234.

JONSSON, I. G. and SKOVGAARD, O. (1978) Wave reflection across a shearing current. *16th Coastal Eng. Conf.* 722-741.

JONSSON, I. G., BRINK-KJAER, O. and THOMAS, G. P. (1978). Wave action and set-down for waves on a shear current. *J. Fluid Mech.* 87, part 3, 401-416.

JONSSON, I. G., SKOVGAARD, O. and WANG, J. D. (1970). Interaction between waves and currents. *Proc. 12th Coastal Eng. Conf.* 1, 489-508.

KEMP, P. H. and SIMONS, R. R. (1982). The interaction of waves and a turbulent current: Waves propagating with the current. *J. Fluid Mech.* 116, 227-250.

KEMP, P. H. and SIMONS, R. R. (1983). The interaction of waves and a turbulent current: Waves propagating against the current. *J. Fluid Mech.* 130, 73-89.

LAMB, H. (1975). *Hydrodynamics. 6th Ed. Cambridge University Press.*

LONGUET-HIGGINS, M. S. (1953). Mass-transport in water waves. *Phil. Trans. Roy. Soc. London, Ser. A* 245, 535—581.

LONGUET-HIGGINS, M. S. and STEWART, R. W. (1960). Changes in the form of short gravity waves on long waves and tidal current. *J. Fluid Mech.* 8, 565—583.

LONGUET-HIGGINS, M. S. and STEWART, R. W. (1961). The changes in amplitude of short gravity waves on steady non-uniform currents. *J. Fluid Mech.* 10, 529—549.

LONGUET-HIGGINS, M. S. and STEWART, R. W. (1964). Radiation stress in water waves, a physical discussion with application. *Deep Sea Res.* 11, 529—562.

PEREGRINE, D.H. (1976). Interaction of water waves and currents. *Adv. Appl. Mech.* 16, 9—117.

SARPKAYA, T. (1957). Oscillatory gravity waves in flowing water. *Trans. Amer. Soc. Civil Eng.* 122, 564—586.

SARPKAYA, T. and ISAACSON, M. (1981). Mechanics of Wave Force on Offshore Structures. *Van Nostrand Reinhold Inc. N. Y.*

SCHUMANN, E. H. (1974). South Africa National Research Institute for Oceanology Internal General Report IG 74/14.

SCHUMANN, E. H. (1975). South Africa Shipping News and Fishing Review, 30(3).

SONG, S. W. and BADDOUR, R. E. (1987). Non-potential wave-current field. *Appl. Math.* 12, 1—11.

SVERDRUP, H. U. (1944). On wave heights in straits and sounds where incoming wave meet a strong tidal current. *Scripps Inst. Ocean wave Rep.* No. 11, 4.

TSAO, S. (1959). Behavior of surface waves on a linearly varying current. *Tr. Mosk. Fiz-Tekh. Inst. Issled. Mekh. Prikl. Mat.* 3, 66—84. (In Russian)

THOMAS, G. P. (1981). Wave-current interactions: An experimental and numerical study. Part 1: Linear waves. *J. Fluid Mech.* 110, 457-474.

UNNA, P. J. I. (1942). Waves and tidal streams. *Nature, Lond.* 149, 219-220.

WHITHAM, G. B. (1962). Mass, momentum and energy flux in water waves. *J. Fluid Mech.* 12, 135-147.

YOON, S. B. and PHILIP L-T. L. (1986). Wave and current interactions in shallow water. *Proc. 20th Coastal Eng. Conf.* 1682-1697.

Further Readings

ASANO, T., NAKAGAWA, M. and IWAGAKI, Y. (1986). Changes in current properties due to wave superimposing. *Proc. 20th Coastal Eng. Conf.* 925—939.

BARBER, N. F. (1949). The behavior of waves on tidal streams. *Proc. Roy. Soc. Ser. A* 198, 81—93.

BENNEY, D. J. (1966). Long nonlinear waves in fluid flows. *J. Math. Phys.* 45, 52—63.

BETTS, P. L. (1970). Waves on a stream of finite depth which has a velocity defect near the free surface. *J. Fluid Mech.* 41, 509—521.

BLYTHE, P. A., KAZAKIA, Y. and VARLEY, E. (1972). The interaction of large amplitude shallow water waves with an ambient shear flow: non-critical flows. *J. Fluid Mech.* 56, 241—255.

BURNS, J. C. (1953). Long waves in running water. *Proc. Cambridge Phil. Soc.* 49, 695—706.

CHANDLER, B. D. and HINWOOD, J. B. (1981). The hydrodynamic forces on submerged horizontal cylinders due to simultaneous wave and current action. *Proc. 5th Australia Conf. on Coastal and Ocean Eng.* 108—115.

CHANDLER, B. D. and HINWOOD, J. B. (1982). Combined wave current forces on horizontal cylinders. *Proc. 18th Coastal Eng. Conf.* 2171—2188.

CRAIK, A. D. D. (1968). Resonant gravity-wave interactions in a shear flow. *J. Fluid Mech.* 34, 531—549.

DEAN, R. G. (1965). Stream function representation of non-linear ocean waves. *J. Geophys. Res.* 70, 4561—4572.

DEAN, R. G. and DALRYMPLE, R. A. (1984). *Water Wave Mechanics for Engineers and Scientists*. Prentice Hall Inc. Englewood Cliffs, New Jersey.

HALES, L. Z. and HERBICH, J. B. (1972). Tidal inlet current-ocean wave interaction. *Proc. 13th Coastal Eng. Conf.* 1, 669-688.

EVANS, D. V. (1975). The transmission of deep water waves across a vortex sheet. *J. Fluid Mech.* 68, 389-401.

FENTON J. D. (1973). Some results for surface gravity waves on shear flows. *J. Inst Math and its Appl.* 12, 1-20.

FISCHER, H. B. FRENCH, R. H. and DELLA, R. (1976). An investigation of possible Cause of the Socalled 'Sneaker Wave' at Tomales Bay, California. *Tech Report No. HEL 28-1, University of California, Berkeley.*

GARGETT, A. E. and HUGHES, B. A. (1972) On the interaction of surface and internal waves. *J. Fluid Mech.* 52, 179-191.

HOLLIDAY, D. (1973). Nonlinear gravity-capillary surface waves in a slowly varying current. *J. Fluid Mech.* 57, 797-802.

HORIKAWA, K., KITAZAWA, O., NAKAI, M. and MIZUGHI, S. (1977). The hydrodynamic forces acting on the cylinder subjected to waves and currents (in Japanese). *Proc. 24th Conf. Coastal Eng. Japan.*

HUIJSMANS, R. H. M. (1986). Wave drift forces in the current. *16th Conf. on Naval Hydrodynamics, Berkely.*

KENYON, K. (1971). Wave refraction in ocean currents. *Deep Sea Res.* 18, 1023-1034.

KNOLL, D. A. and HERBICH, J. B. (1980). Wave and current forces on a submerged offshore pipeline. *Pro. of 12th Offshore Technology Conf. 1 Paper No. 3762.*

KOBAYASHI, M. (1981). On the hydrodynamic forces and moments acting on a three dimensional body with a constant forward speed (in Japanese). *J. Society of Naval Architects, Japan,* 175-189.

KOTERAYAMA, W. (1984). Wave forces acting on a vertical circular cylinder with a constant forward velocity. *Ocean Eng.* 11 363-379.

LEWIS, J. E. LAKE, B. M. and KO, D. R. S. (1974). On the interaction of internal waves and surface gravity waves. *J. Fluid Mech.* 63, 773-800.

MALLORY, J. K. (1974). Abnormal Waves on the South East Coast of South Africa, *Int. Hydrographic Review*: 51, 99—129.

MCKEE, W. D. (1974). Waves on a shearing current: a uniformly valid asymptotic solution. *Proc. Cambridge Phil Soc.* 75, 295—301.

MEI, C. C. (1982). The Applied Dynamics of Ocean Waves. *John Wiley and Sons Inc. N. Y.*

MES, M. J. (1977). Current can influence wave properties. *Petroleum Engineer Oct.* 62—68.

PEREGRINE, D. H. (1968). Long waves in uniform channel of arbitrary cross-section. *J. Fluid Mech.* 32, 353—365.

PEREGRINE, D. H. and SMITH, R. (1975). Stationary gravity waves on non-uniform free streams jet-like flows. *Math. Proc. Cambridge Phil. Soc.* 77, 415—438.

SEKITA, K. (1975). Laboratory experiments on wave and current forces acting on a fixed platform. *Proc. of the Offshore Technology Conf.* 1 Paper No. 2191.

SHEMDIN, O. H. (1972). Wind-generated current and phase speed of wind waves. *J. Phys. Oceanogr.*, 2, 411—419.

SKOP, R. A. (1987). Approximate Dispersion Relation For Wave-current Interaction. *J. of Waterway, Port, Coastal, and Ocean Eng.* 113, No. 2, 187—196.

SLEATH, J. F. A. (1973). Mass transport in water waves of very small amplitude. *J. Hydraul. Res.* 11, 369—383.

SMITH, R. (1975). The reflection of short gravity waves on a non-uniform current. *Math. Proc. Cambridge Phil. Soc.* 78, 517—525.

THOMSON, J. A. and WEST, B. J. (1975). Interaction of small amplitude surface gravity waves with surface currents *J. Phys. Oceanog.* 5, 736—749.

TUNG C. C. and HUANG, N. E. (1973). Combined effects of current and waves on fluid force. *Ocean Eng.* 2, 183—193.

TUNG C. C. and HUANG, N. E. (1973). Influence of wave-current interaction on fluid force. *Ocean Eng.* 2, 207-218.

VENEZIAN, G. (1979). Hydrodynamic wave-current pressure. *Technical Report No. 46, University of Hawaii.*

YIH, C. S. (1972). Surface waves in flowing water. *J. Fluid Mech.* 51, 209-220.

Appendix A

A Discussion on the Radiation Stress and Energy Transfer in a wave-current Field

The term "radiation stress", was coined and introduced by Longuet-Higgins and Stewart (1961, 1962, 1964). In a one dimensional case, the product US_x , was defined to be the rate of work done by the current on the wave, where S_x represents the radiation stress and U the current speed. The radiation stress S_x was defined when considering the mean energy flux to the second order of wave amplitude a across a vertical plane normal to the combined wave-current propagating direction. In this appendix the expression of the mean energy flux in a wave-current field is reconsidered.

The mean energy flux in a wave-current field is defined as (see section 4.2.3)

$$E_{wc} = \frac{1}{2\pi} \int_0^{2\pi} \int_{-d}^{\eta} \left\{ P + \frac{1}{2} \rho \left[\left(\frac{\partial \Phi}{\partial x} \right)^2 + \left(\frac{\partial \Phi}{\partial z} \right)^2 \right] + \rho g z \right\} \frac{\partial \Phi}{\partial x} dx d\theta \quad (\text{A.1})$$

For the irrotational wave-current field Φ of pressure distribution $P(z)$ and mean water depth d , the periodical surface disturbance is denoted by $\eta(x, t)$.

Substituting the second order P and Φ from equations (3.73), (3.61) respectively into the above definition and using the following properties

$$\int_0^{2\pi} \cos \theta d\theta = 0 \quad (\text{A.2})$$

$$\int_0^{2\pi} \cos 2\theta d\theta = 0 \quad (\text{A.3})$$

the mean energy flux across a vertical plane in the wave-current field E_{wc} becomes

$$E_{wc} = \frac{1}{2\pi} \int_{-d}^{\eta} \left[\rho a A \sigma \cosh K(z+d) \cos \theta + \frac{1}{2} \rho g K \frac{a^2}{\sinh 2Kd} + \frac{1}{2} \rho U^2 \right] [U + aAK \cosh K(z+d) \cos \theta] dx d\theta \quad (\text{A.4})$$

where

$$\sigma = KU + \sigma_r,$$

$$\sigma_r = [gK \tanh Kd]^{1/2},$$

$$\theta = Kx - \sigma t,$$

$$A = [g/(K \sinh Kd \cosh Kd)]^{1/2}.$$

Substituting $\sigma = KU + \sigma_r$ into (A.4) E_{wc} takes the form

$$\begin{aligned} E_{wc} = & \frac{1}{2\pi} \int_0^{2\pi} \int_{-d}^d [\rho a A \sigma_r \cosh K(z+d) \cos \theta + \\ & + \rho a AKU \cosh K(z+d) \cos \theta + \\ & + \frac{1}{2} \rho g K \frac{a^2}{\sinh 2Kd} + \frac{1}{2} \rho U^2 \\ & [U + aAK \cosh K(z+d) \cos \theta] dz d\theta \end{aligned} \quad (A.5)$$

Now, expression (A.5) is expressed as the following sum

$$E_{wc} = E_1 + E_2 + E_3 + E_4 + E_5 + E_6 \quad (A.6)$$

where

$$E_1 = \frac{1}{2\pi} \int_0^{2\pi} \int_{-d}^d \frac{1}{2} \rho U^2 U dz d\theta \quad (\text{A.7})$$

or

$$E_1 = \frac{1}{2} \rho U^2 U \quad \text{to } O(Ka^2) \quad (\text{A.8})$$

$$E_2 = \frac{1}{2} \int_0^{2\pi} \int_{-d}^d \rho a^2 A^2 \sigma_r K \cosh^2 K(z+d) \cos^2 \theta dz d\theta \quad (\text{A.9})$$

or

$$E_2 = \frac{1}{2} \rho g a^2 \frac{1}{2} \left(1 + \frac{2Kd}{\sinh 2Kd}\right) C_r \quad \text{to } O(Ka^2) \quad (\text{A.10})$$

$$E_3 = \frac{1}{2\pi} \int_0^{2\pi} \int_{-d}^d \frac{1}{2} \rho U^2 a A K \cosh K(z+d) \cos \theta dz d\theta \quad (\text{A.11})$$

or

$$E_3 = \frac{1}{2} \rho U^2 d \frac{1}{2} \frac{a^2 g}{C_r d} \quad (\text{A.12})$$

$$E_4 = \frac{1}{2\pi} \int_0^{2\pi} \int_{-d}^d U \rho a A \sigma_r \cosh K(z+d) \cos \theta dz d\theta \quad (\text{A.13})$$

or

$$E_4 = U \frac{1}{2} \rho g a^2 \quad (\text{A.14})$$

From the expressions of E_1 , E_2 , E_3 , and E_4 it can be seen that

$$E_1 = E_U U \quad (\text{A.15})$$

represents the current energy transported by the current itself, where $E_U = \frac{1}{2} \rho d U^2$ is the current energy density.

$$E_2 = E_w C_{gr} \quad (\text{A.16})$$

represents the wave energy transported by the wave itself in still water, where $E_w = \frac{1}{2} \rho g a^2$ is the wave energy density per unit area if no current is present, and $C_{gr} = \frac{1}{2} (1 + \frac{2Kd}{\sinh 2kd}) C_r$ is the relative wave group velocity.

$$E_3 = E_U u_w \quad (\text{A.17})$$

represents the current energy transported by the wave because of the wave drift velocity $u_w = \frac{1}{2} \frac{a^2 g}{C_r d}$.

$$E_4 = E_w U \quad (\text{A.18})$$

represents the wave energy transported by the current U .

E_5 and E_6 are the results of the nonlinear interaction of the wave and the current. They are given as

$$E_5 = \frac{1}{2\pi} \int_0^{2\pi} \int_{-d}^0 [\rho a A K U \cosh K(z+d) \cos \theta + \frac{1}{2} \rho g K a^2 \frac{1}{\sinh 2Kd}] U dz d\theta \quad (\text{A.19})$$

and

$$E_6 = \frac{1}{2\pi} \int_0^{2\pi} \int_{-d}^0 \rho a^2 A^2 K^2 U \cosh^2 K(z+d) \cos^2 \theta dz d\theta \quad (\text{A.20})$$

Performing the integrations yields

$$E_s = \frac{1}{2} \frac{\rho g}{C_r d} \rho U^2 d + \frac{1}{2} \rho \eta K \alpha^2 \frac{U d}{\sinh 2Kd} \quad (\text{A.21})$$

and

$$E_0 = \frac{1}{2} \rho g \alpha^2 \frac{1}{2} \left(1 + \frac{2Kd}{\sinh 2Kd} \right) U \quad (\text{A.22})$$

Adding E_s and E_0 gives

$$E_{s0} = \frac{1}{2} \frac{\rho g}{C_r d} \rho U^2 d + \frac{1}{2} \rho g \alpha^2 \left(\frac{1}{2} + \frac{2Kd}{\sinh 2Kd} \right) U \quad (\text{A.23})$$

or

$$E_{s0} = u_w S_r + U S_x \quad (\text{A.24})$$

where $S_x = \frac{1}{2} \rho g \alpha^2 \left(\frac{1}{2} + \frac{2Kd}{\sinh 2Kd} \right)$ is the so called radiation stress (Longuet-Higgins 1961), and $S_r = \rho d U^2 = 2E_U$.

Now it is clear that $E_{s0} = E_s + E_0$ is a part of E_{we} , hence an energy flux too. If $U S_x$ is considered to be the work done by the current on the wave, there is no reason not to define $u_w S_R$ as the work done by the wave on the current.

Appendix B

Numerical Considerations and Precision Control

The wave length L , wave height H , water depth d , and current speed U of the combined wave-current field are computed by solving numerically the system of equations (4.61), (4.62), (4.63), and (4.64). The numerical method is based on Newton's method. The algorithm is discussed below.

Assuming the system of n equations in n variables is given as

$$f_1(x_1, x_2, \dots, x_n) = 0$$

$$f_2(x_1, x_2, \dots, x_n) = 0$$

(B.1)

$$f_n(x_1, x_2, \dots, x_n) = 0$$

where f_i ($i = 1, 2, \dots, n$) are nonlinear functions of x_i ($i = 1, 2, \dots, n$). The solutions of the following single equation which is formed from f_i namely

$$F = \sum_{i=1}^n f_i^2(x_1, x_2, \dots, x_n) = 0. \quad (B.2)$$

is considered to satisfy the system of equations (B.1).

Therefore the problem of finding the solution of the system (B.1) could be converted into that of finding the solution of the single equation (B.2). The numerical solution of equation (B.2) could be computed by directly using Newton's method.

On solving equation (B.2) the precision is controlled by letting $F \leq \delta$, with δ given any preassigned small value. In the computations of this thesis δ was of the order 1.0×10^{-20} . The computation program was running in four time precision.

The problem of controlling the precision of the individual variables x_i ($i = 1, 2, \dots, n$) in (B.2) is to be noted. The precision controlling parameter δ controls only the accuracy of F and not of X_i , which are assumed to be the approximate solutions of the variables x_i . The precision of X_i could therefore be less than the precision of f_i , which is the order of $\frac{1}{2}\delta$. Hence the convergence of the individual solutions X_i should also be tested to ensure the accuracy requirement.

In this thesis the testing on the precision of the individual X_i was carried out in an adhoc manner by resolving the system several times and checking the convergence of X_i . Repeating the calculation respectively with $\delta = 1.0 \times 10^{-16}$, $\delta = 1.0 \times 10^{-18}$, $\delta = 1.0 \times 10^{-20}$ the results of X_i were compared. In all the computations the number of accurate digits are found to be not less than 5 decimal digits.

Appendix C

Computer Program

In this appendix the listing of the FORTRAN program used in the calculations pertinent to this thesis is presented. This program includes five subroutines and one function subprogram. Subroutine SNSE1 and function FNC are used to calculate numerically the four variables W , X , Y , Z in the nonlinear system of equations (4.61) — (4.64). Subroutine WAVE is designed to calculate the wave height H , wave length L , water depth d , and current speed U of the combined wave-current field by using W , X , Y , Z . Subroutine VELOCITY is used to calculate the particle velocity and acceleration of the combined wave-current field by using L , H , d , and U . Subroutines PATH1 and PATH2 are used to calculate the path of a particle in the combined wave-current field.

The program was debugged and run on the VAX 8530 of the Faculty of Engineering at M. U. N. The program is listed below.

Flowchart



C
C

A PROGRAM OF W-C INTERACTION CALCULATION

```
IMPLICIT REAL* 16 (A-H,O-Z)
DIMENSION X(4),HX(99),DF(99),F(99),G(99),E(99),
1 H(99),O(99),R(99),Q(99),S(99),F2(99),G2(99),
1 T(99),U(99),CU(99),VELOWX(99),VELOWY(99),Z(30),
1 Y(99),WK(99),CH(99),SH(99),VELOX(99),VELOY(99),
1 VELOX1(55),VELOX2(55),VELOY1(55),VELOY2(55)
DIMENSION AAW2(99),AA1(99),AA2(99),XX2(99,99),
1 XX1(99,99),AA1S(99),WK2(55),SH2(55),CH2(55),
1 AX1(44),AX2(44),AX(44),AY1(44),AY2(44),AY(44),-
1 XP(300),YP(300),XD(300),YD(300),XX3(99,99)
```

```
OPEN (UNIT=30, FILE='PROWAVE.RES', STATUS='NEW')
OPEN (UNIT=60, FILE='PROWAVE.RES', STATUS='NEW')
OPEN (UNIT=40, FILE='PROWAVE.DAT', STATUS='OLD')
```

```
120 READ(40,*) WL0,WH0,D0,U0
B=1.0D-20
HB=1.0D-12
c B=Precision control parameter.
c HB=Iteration step length.
```

```
X1=-0.10
X2=1.0
X3=1.0D-2
X4=1.0
c Given the initial guess values.
```

```
1 CALL WAVE(A1,A2,A3,X1,X2,X3,X4,
WL0,D0,WH0,WL,WH,DN,U,WCO)
A1=(WH0/(2.0*D0))**2
```

```
A2=U0/WC0
A3=WL0/D0
WRITE(30,55)
55 FORMAT(3x,4hWL0=,f15.7,3x,4hWH0=,f15.7,
1 3x,3hD0=,f15.7)
WRITE(30,65)
65 FORMAT(3x,3hA1=,f15.7,4x,3hA2=,f15.7,
1 4x,3hA3=,f15.7)
```

```
CALL SNSE1(B,HB,A1,A2,A3,X1,X2,X3,X4)
CALL WAVE(A1,A2,A3,X1,X2,X3,X4,WL0,
1 DO,WH0,WL,WH,D,UH,WC0)
CALL VELOCITY(D0,D,WL,UH,WH,
1 VELOX,VELOY,WC0,WH0)
```

```
X0=0.0
Z0=-5.0
c (X0,Z0) is the particle initial location.
```

```
CALL PATH1(D,WH,WL,UH,X0,Z0,30)
```

```
X0=0.0
Z0=-20.0
```

```
CALL PATH2(D,WH,WL,UH,X0,Z0,60)
```

```
GO TO 120
C STOP
END
```

```

FUNCTION FNC(A1,A2,A3,X1,X2,X3,X4)
IMPLICIT REAL*16 (A-H,O-Z)
DIMENSION X(4),A(3),F(99),G(99),E(99),H(99),O(99),
1 R(99),P(99),Q(99),S(99),F2(99),G2(99),T(99),U(99)

```

```

I=1

```

```

C      WRITE (30,170) X1,X2,X3,X4,A1,A2,A3
C 170  FORMAT (1X,7F13.4)
c      For checking the iterating results.

```

```

F(I)=6.28318/A3
F1=F(I)

```

```

G(I)=6.28318*X4/(A3*X2)
F2(I)=F(I)*2.0
G2(I)=G(I)*2.0

```

```

E(I)=SQRT((EXP(F(I))-EXP(-F(I)))/(EXP(F(I))+EXP(-F(I))))
H(I)=SQRT((EXP(G(I))-EXP(-G(I)))/(EXP(G(I))+EXP(-G(I))))
O(I)=(EXP(F(I))-EXP(-F(I)))*0.5
P(I)=(EXP(F(I))+EXP(-F(I)))*0.5
Q(I)=(EXP(G(I))-EXP(-G(I)))*0.5
R(I)=(EXP(G(I))+EXP(-G(I)))*0.5
T(I)=(EXP(G2(I))-EXP(-G2(I)))*0.5
U(I)=(EXP(F2(I))-EXP(-F2(I)))*0.5

```

```

E1=E(I)
G1=G(I)
H1=H(I)
O1=O(I)
P1=P(I)
Q1=Q(I)
S1=S(I)

```

$$FNC1=X1+X2*H(I)/E(I)-X2*X2$$

$$FNC2=A3*X4*X1+3.14*X3/(X2*E(I)*H(I))$$

$$1 -A2*A3-3.14*A1/E(I)**2$$

$$FNC3=X4**2+X3*(0.5+2.0*3.14*X4/(A3*X2**2*Q(I)*R(I)))$$

$$1 +A3*X1**2*X4*E(I)**2/3.14$$

$$1 +2.0*X1*X3*E(I)/(X2*H(I))-1.0$$

$$1 -A1*(0.5+2.0*3.14/(A3*O(I)*P(I)))$$

$$1 -A3*A2**2*E(I)**2/3.14$$

$$FNC41=A3*X4*X1**3*E(I)**2/3.14$$

$$1 +3.0*X3*X1**2*E(I)/(X2*H(I))$$

$$1 +X3*X2*H(I)*(1.0+2.0*3.14*X4$$

$$1 /(A3*X2**2*Q(I)*R(I)))/E(I)$$

$$1 +X3*X1*(3.0+4.0*3.14*X4$$

$$1 /(A3*X2**2*Q(I)*R(I)))$$

$$FNC42=A3*A2**3*E(I)**2/3.14159$$

$$1 +A1*(1.0+2.0*3.14/(A3*O(I)*P(I)))$$

$$FNC4=FNC41-FNC42$$

$$FNC=FNC1**2+FNC2**2+FNC3**2+FNC4**2.$$

C* WRITE(30,110) FNC
C 110 FORMAT(1X,1D25.9)
c For precision control.

RETURN
END

```
SUBROUTINE SNSE1(B,HB,A1,A2,A3,X1,X2,X3,X4)
IMPLICIT REAL*16 (A-H,O-Z)
DIMENSION X(4),HX(4),DF(4),A(4),F(100),G(100),
1 E(100),H(100),O(100),R(100),P(100),Q(100),
1 F2(99),G2(99),T(99),U(99)
```

```
I=1
```

```
C WRITE (30,200) B,HB
C 200 FORMAT (1X,2E15.7)
c Looking at the increment direction.
```

```
7 X(1)=X1
X(2)=X2
X(3)=X3
X(4)=X4
```

```
C WRITE(30,160) (X(L),L=1,4)
C 160 FORMAT(1X,4F9.3)
c Checking the convergent speed.
```

```
DO 11 L=1,4
IF(X(L)) 15,2,15
2 HX(L)=HB
GO TO 11
15 HX(L)=HB*X(L)
11 CONTINUE
X1=X(1)
X2=X(2)
X3=X(3)
X4=X(4)
```

F1=FNC(A1,A2,A3,X1,X2,X3,X4)

IF(F1-B) 3,3,4

SUM=0.0

X(1)=X1

X(2)=X2

X(3)=X3

X(4)=X4

DO 22 L=1,4

X(L)=X(L)+HX(L)

X1=X(1)

X2=X(2)

X3=X(3)

X4=X(4)

FH=FNC(A1,A2,A3,X1,X2,X3,X4)

X(1)=X1

X(2)=X2

X(3)=X3

X(4)=X4

DF(L)=(FH-F1)/HX(L)

SUM=SUM+DF(L)*DF(L)

22 X(L)=X(L)-HX(L)

RLMT=F1/SUM

X1=X(1)-RLMT*DF(1)

X2=X(2)-RLMT*DF(2)

X3=X(3)-RLMT*DF(3)

X4=X(4)-RLMT*DF(4)

GO TO 7

3 RETURN

END

```

SUBROUTINE WAVE(A1,A2,A3,X1,X2,X3,X4,
1  WLO,D0,WH0,WL,WH,DN,U,WCO)
IMPLICIT REAL*16 (A-H,O-Z)
WL=X2*X2*WLO
WH=2.0*D0*SQRT(X3)
D=D0*X4
DK=6.28*D0/WLO
TH=(EXP(DK)-EXP(-DK))/(EXP(DK)+EXP(-DK))
WCO=SQRT(9.8*WLO/6.28*TH)
U=X1*WCO,
WLBWLO=X2*X2
WHBWH0=SQRT(X3/A1)
DBD0=X4
DELTD=(D0-D)/D0
DN=D0+(D0-D)
U0=A2*WCO
DELTU=(A2-X1)
WL=WLBWLO*WLO
WH=WHBWH0*WH0

WRITE(30,98)
98  FORMAT(10X,2hWL,10X,2hWH,10X,1hU,12X,1hD)

WRITE(30,99) WL,WH,U,D
99  FORMAT(5X,4F12.5)

RETURN
END

```

```

SUBROUTINE VELOCITY(D0,D,WL,U,
1 WH,VELOX,VELOY,WCO,WHO)
IMPLICIT REAL*16 (A-H,O-Z)
DIMENSION Y(99),WK(99),CH(99),SH(99),VELOX(99),
1 VELOY(99),CU(99),VELOWX(99),VELOWY(99),VEXBC(99),
1 VEYBC(99),DB(99),Z(30),VELOX1(55),VELOX2(55),
1 VELOY1(55),VELOY2(55),WK2(55),SH2(55),CH2(55),
1 AX1(44),AX2(44),AX(44),AY1(44),AY2(44),AY(44)

```

```

WKD=6.28*D/WL
SH1=(EXP(WKD)-EXP(-WKD))*0.5
CH1=(EXP(WKD)+EXP(-WKD))*0.5
TH=SH1/CH1
WKD2=2.0*WKD
SH11=(EXP(WKD2)-EXP(-WKD2))*0.5
CH11=(EXP(WKD2)+EXP(-WKD2))*0.5
U1=U/D0
SIGMA=SQRT(2.0*3.14*9.8*TH/WL)

```

```

Y(0)=0.0
Z(0)=-1.0

```

```

DO 10 I=1,20
Y(I)=D/20*I
Z(I)=-(1.0-0.05*I)
10 CONTINUE

```

```

DO 100 I=0,20
WK(I)=6.28*Y(I)/WL
WK2(I)=2.0*WK(I)
CH(I)=(EXP(WK(I))+EXP(-WK(I)))/2.0

```

```

SH(I)=(EXP(WK(I))-EXP(-WK(I)))/2.0
CH2(I)=(EXP(WK2(I))+EXP(-WK2(I)))/2.0
SH2(I)=(EXP(WK2(I))+EXP(-WK2(I)))/2.0
VELOX1(I)=U+9.8*3.14*WH*CH(I)/(SIGMA*CH1*WL)
VELOY1(I)=3.14*9.8*SH(I)*WH/(SIGMA*WL*CH1)
VELOX2(I)=(3.0*3.14159)/8.0*WH**2*SIGMA
1 /(WL*SH1**4)*CH2(I)
VELOY2(I)=(3.0*3.14159)/8.0*WH**2*SIGMA
1 /(WL*SH1**4)*SH2(I)
VELOX(I)=VELOX1(I)+VELOX2(I)
VELOY(I)=VELOY1(I)+VELOY2(I)
VEXBC(I)=VELOX(I)/WC0
VEYBC(I)=VELOY(I)/WC0
DB(I)=(D/SQRT(9.8*WH0))/10*I
AX1(I)=9.8*3.14159*WH*CH(I)/(WL*CH1)
AX2(I)=0.5*((3.0*3.14159/4.0)*WH**2
1 *SIGMA**2*CH2(I)/(WL*SH1**4)
1 -9.8*WH**2*3.14159**2/(WL**2*SH11))
AX(I)=AX1(I)+AX2(I)
AY1(I)=9.8*3.14159*WH*SH(I)/(WL*CH1)
AY2(I)=9.8*3.14159**2*WH**2*SH2(I)/(SH11*WL**2)
1 -(3.0*3.14159/4.0)*WH**2*SIGMA**2*SH2(I)/(WL*SH1**4)
AY(I)=AY1(I)+AY2(I)

WRITE(30,200) ax(I),Z(I)
200 FORMAT(7X,2F15.7)
WRITE(60,201) ay(I),Z(I)
201 FORMAT(7X,2F15.7)

100 CONTINUE
RETURN
END

```

```
SUBROUTINE PATH1(D,WH,WL,U,X0,Z0,OP)
IMPLICIT REAL*16(A-H,O-Z)
DIMENSION XP(300),YP(300),XD(300),YD(300)
```

```
WKD=6.28318*D/WL
SH=(EXP(WKD)-EXP(-WKD))*0.5
CH=(EXP(WKD)+EXP(-WKD))*0.5
TH=SH/CH
SIGMAR=SQRT(6.28318*9.8*TH/WL)
TR=6.28318/SIGMAR
WKZ=6.28318*(Z0+D)/WL
SHZ=(EXP(WKZ)-EXP(-WKZ))*0.5
CHZ=(EXP(WKZ)+EXP(-WKZ))*0.5
THZ=SHZ/CHZ
ALF=0.5*WH*CHZ/SH
BET=0.5*WH*SHZ/SH
```

```
C WRITE(30,20) ALF,BET
C 20 FORMAT(5X,2F15.7)
```

```
DO 50 I=0,60
T=TR/30.0*I
XP(I)=X0+U*T-ALF*SIN(-SIGMAR*T)
YP(I)=Z0+BET*COS(-SIGMAR*T)
XD(I)=XP(I)/D
YD(I)=YP(I)/D
```

```
WRITE(30,55) XD(I),YD(I)
55 FORMAT(1X,2F15.7)
```

```
50 CONTINUE
RETURN
END
```

```
SUBROUTINE PATH2(D,WH,WL,U,X0,Z0,OP)
IMPLICIT REAL*16(A-H,O-Z)
DIMENSION XP(300),YP(300),XD(300),YD(300)
```

```
WKD=6.28318*D/WL
SH=(EXP(WKD)-EXP(-WKD))*0.5
CH=(EXP(WKD)+EXP(-WKD))*0.5
TH=SH/CH
SIGMAR=SQRT(6.28318*9.8*TH/WL)
TR=6.28318/SIGMAR
WKZ=6.28318*(Z0+D)/WL
SHZ=(EXP(WKZ)-EXP(-WKZ))*0.5
CHZ=(EXP(WKZ)+EXP(-WKZ))*0.5
THZ=SHZ/CHZ
ALF=0.5*WH*CHZ/SH
BET=0.5*WH*SHZ/SH
DO 50 I=0,60
T=TR/30.0*I
XP(I)=X0+U*T-ALF*SIN(-SIGMAR*T)
YP(I)=Z0+BET*COS(-SIGMAR*T)
XD(I)=XP(I)/D
YD(I)=YP(I)/D
```

```
WRITE(60,55) XD(I),YD(I)
55 FORMAT(1X,2F15.7)
```

```
50 CONTINUE
RETURN
END
```

Appendix D

Some Numerical Results

In this appendix some numerical results are presented. Tables (D.1), (D.2), (D.3), and (D.4) give the wave length ratio L/L_0 , wave height ratio H/H_0 , current ratio $(U - U_0)/C_0 \times 10^{-4}$ and water depth ratio $(d - d_0)/d_0 \times 10^{-4}$ respectively for various values of the parameter U_0/C_0 . When the current-free wave and the wave-free current before the interaction are known the changes in wave length, wave height, current speed and water depth can be directly find from tables (D.1) — (D.4), for the shown range of the parameters.

Table (D.1) Numerical results of wave length ratio L/L_0

L_0/d_0	H_0/L_0	U_0/C_0	-0.15	-0.10	-0.05	0.00	0.05	0.10	0.15	0.20
24	0.00053		0.84561	0.89733	0.94877	1.00000	1.05105	1.10197	1.15276	1.20346
	0.00091		0.84557	0.89731	0.94876	1.00000	1.05106	1.10198	1.15277	1.20348
	0.00129		0.84551	0.89728	0.94875	1.00000	1.05107	1.10199	1.15280	1.20350
	0.00149		0.84547	0.89726	0.94874	1.00000	1.05108	1.10200	1.15281	1.20352
16	0.00079		0.84018	0.89404	0.94727	1.00000	1.05234	1.10436	1.15611	1.20766
	0.00137		0.84014	0.89402	0.94726	1.00000	1.05235	1.10437	1.15613	1.20767
	0.00194		0.84008	0.89399	0.94725	1.00000	1.05235	1.10439	1.15616	1.20770
	0.00224		0.84004	0.89396	0.94724	1.00000	1.05236	1.10440	1.15617	1.20772
10	0.00127		0.82527	0.88511	0.94321	1.00000	1.05577	1.11072	1.16502	1.21879
	0.00219		0.82522	0.88509	0.94320	1.00000	1.05577	1.11074	1.16504	1.21881
	0.00310		0.82514	0.88505	0.94319	1.00000	1.05579	1.11076	1.16507	1.21884
	0.00358		0.82508	0.88502	0.94318	1.00000	1.05579	1.11077	1.16509	1.21886
4	0.00317		0.73023	0.82984	0.91853	1.00000	1.07631	1.14874	1.21815	1.28514
	0.00548		0.72997	0.82974	0.91850	1.00000	1.07633	1.14877	1.21819	1.28519
	0.00775		0.72957	0.82959	0.91845	1.00000	1.07636	1.14882	1.21825	1.28526
	0.00895		0.72930	0.82949	0.91841	1.00000	1.07638	1.14885	1.21829	1.28531

Table (D.2) Numerical results of wave height ratio H/H_0 .

L_0/d_0	H_0/L_0	U_0/C_0	-0.15	-0.10	-0.05	0.00	0.05	0.10	0.15	0.20
24	0.00053		1.28395	1.15954	1.07029	1.00000	0.93862	0.87914	0.81604	0.74424
	0.00091		1.26565	1.15464	1.06973	1.00000	0.93911	0.88293	0.82847	0.77335
	0.00129		1.26112	1.15346	1.06960	1.00000	0.93925	0.88386	0.83154	0.78044
	0.00149		1.26003	1.15318	1.06958	1.00000	0.93925	0.88409	0.83229	0.78220
16	0.00079		1.29890	1.16692	1.07319	1.00000	0.93661	0.87568	0.81152	0.73893
	0.00137		1.28038	1.16199	1.07263	1.00000	0.93710	0.87946	0.82389	0.76789
	0.00194		1.27581	1.16080	1.07251	1.00000	0.93721	0.88039	0.82694	0.77495
	0.00224		1.27472	1.16052	1.07248	1.00000	0.93724	0.88061	0.82770	0.77669
10	0.00127		1.34050	1.18680	1.08086	1.00000	0.93143	0.86683	0.80002	0.72550
	0.00219		1.32144	1.18182	1.08030	1.00000	0.93191	0.87056	0.81222	0.75403
	0.00310		1.31678	1.18062	1.08018	1.00000	0.93202	0.87148	0.81522	0.76097
	0.00358		1.31568	1.18035	1.08014	1.00000	0.93204	0.87169	0.81596	0.76269
4	0.00317		1.58871	1.29008	1.11808	1.00000	0.90775	0.82710	0.74926	0.66740
	0.00548		1.56829	1.28521	1.11758	1.00000	0.90817	0.83038	0.75992	0.69226
	0.00775		1.56423	1.28426	1.11753	1.00000	0.90825	0.83116	0.76252	0.69829
	0.00895		1.56376	1.28415	1.11755	1.00000	0.90825	0.83133	0.76314	0.69976

Table (D.3) Numerical results of current velocity change ratio

$$[(U - U_0)/C_0] \times 10^{-4}$$

L_0/d_0	H_0/L_0	U_0/C_0	-0.15	-0.10	-0.05	0.00	0.05	0.10	0.15	0.20
24	0.00053		-0.15298	-0.07698	-0.03110	0.00000	0.02382	0.04422	0.06318	0.08152
	0.00091		-0.42401	-0.22300	-0.09253	0.00000	0.07093	0.12917	0.17979	0.22567
	0.00129		-0.83093	-0.44215	-0.18471	0.00000	0.14162	0.25662	0.35474	0.44192
	0.00149		-1.10246	-0.58835	-0.24619	0.00000	0.18876	0.34161	0.47139	0.58610
16	0.00079		-0.16637	-0.08330	-0.03355	0.00000	0.02557	0.04736	0.06753	0.08702
	0.00137		-0.46271	-0.24169	-0.09986	0.00000	0.07617	0.13850	0.19256	0.24156
	0.00194		-0.90765	-0.47942	-0.19936	0.00000	0.15209	0.27523	0.38015	0.47340
	0.00224		-1.20457	-0.63800	-0.26573	0.00000	0.20272	0.36641	0.50523	0.62799
10	0.00127		-0.20756	-0.10203	-0.04064	0.00000	0.03047	0.05604	0.07942	0.10189
	0.00219		-0.58192	-0.29711	-0.12105	0.00000	0.09083	0.16430	0.22756	0.28470
	0.00310		-1.14412	-0.58995	-0.24173	0.00000	0.18140	0.32673	0.44980	0.55895
	0.00358		-1.51928	-0.78533	-0.32222	0.00000	0.24180	0.43504	0.59799	0.74182
4	0.00317		-0.65398	-0.27335	-0.09986	0.00000	0.06749	0.11932	0.16332	0.20351
	0.00548		-1.88354	-0.80579	-0.29840	0.00000	0.20173	0.35291	0.47582	0.58241
	0.00775		-3.73721	-1.60619	-0.59657	0.00000	0.40320	0.70346	0.94473	1.15092
	0.00895		-4.97927	-2.14097	-0.79559	0.00000	0.53759	0.93725	1.25744	1.53003

Table (D.4) Numerical results of water depth change ratio

$$[(d - d_0)/d_0] \times 10^{-4}$$

L_0/d_0	H_0/L_0	U_0/C_0	-0.15	-0.10	-0.05	0.00	0.05	0.10	0.15	0.20
24		0.00053	0.12602	0.05811	0.02133	0.00000	-0.01396	-0.02519	-0.03665	-0.05037
		0.00091	0.33681	0.16437	0.06294	0.00000	-0.04106	-0.06964	-0.09153	-0.11055
		0.00129	0.65330	0.32387	0.12539	0.00000	-0.08173	-0.13633	-0.17387	-0.20084
		0.00149	0.86449	0.43028	0.16705	0.00000	-0.10884	-0.18080	-0.22878	-0.26104
16		0.00079	0.12339	0.05610	0.02032	0.00000	-0.01298	-0.02321	-0.03359	-0.04611
		0.00137	0.33007	0.15867	0.05996	0.00000	-0.03814	-0.06390	-0.08304	-0.09931
		0.00194	0.64039	0.31264	0.11944	0.00000	-0.07589	-0.12496	-0.15723	-0.17912
		0.00224	0.84748	0.41535	0.15911	0.00000	-0.10107	-0.16567	-0.20670	-0.23233
10		0.00127	0.11701	0.05103	0.01777	0.00000	-0.01051	-0.01826	-0.02600	-0.03560
		0.00219	0.31374	0.14426	0.05239	0.00000	-0.03081	-0.04959	-0.06197	-0.07152
		0.00310	0.60920	0.28421	0.10435	0.00000	-0.06127	-0.09661	-0.11593	-0.12541
		0.00358	0.80642	0.37759	0.13901	0.00000	-0.08159	-0.12797	-0.15192	-0.16154
4		0.00317	0.09805	0.02940	0.00660	0.00000	-0.00009	-0.00280	-0.00600	-0.00842
		0.00548	0.26952	0.08297	0.01928	0.00000	-0.00068	-0.01125	-0.02677	-0.04455
		0.00775	0.52807	0.16351	0.03833	0.00000	-0.00156	-0.02393	-0.05795	-0.09877
		0.00895	0.70134	0.21733	0.05105	0.00000	-0.00215	-0.03238	-0.07875	-0.13493



